R. & M. No. 2628
(11,476, 12,193)
A.R.C. Technical Report

MINISTRY OF SUPPLY

AERONAUTICAL RESEARCH COUNCIL
REPORTS AND MEMORANDA

Boundary-Layer Flow along a Flat Plate with Uniform Suction

By

J. M. Kay, M.A., A.M.I.Mech.E.,
Cambridge University Engineering Laboratory

LONDON: HER MAJESTY'S STATIONERY OFFICE
1953
PRICE 7*s.* 6*d.* NET

Boundary-Layer Flow along a Flat Plate with Uniform Suction

By

J. M. KAY, M.A., A.M.I.Mech.E.

CARRIED OUT AT THE CAMBRIDGE UNIVERSITY ENGINEERING LABORATORY.

Presented by SIR MELVILL JONES, F.R.S.

Reports and Memoranda No. 2628

May, 1948

Summary.—Experiments have been carried out in the closed-circuit wind-tunnel at Cambridge University to determine the effectiveness of distributed suction as a means of controlling and stabilizing the flow in a boundary layer. These experiments have shown that the laminar exponential suction profile can be established and retained, provided the boundary layer is in an undisturbed laminar condition at the start of the suction region. Good agreement has been obtained between the measured velocity profiles and the theoretical exponential form. It has also been shown that the laminar suction profile, when once established, is able to surmount small disturbances which would normally be sufficient to promote transition in the absence of suction. There is, however, no evidence whatever to suggest that laminar flow can be re-established if transition once occurs.

The variation with rate of suction of the total effective drag of a flat plate has been investigated. It has been established that, from the point of view of drag reduction, the optimum rate of suction is the minimum rate which is sufficient to maintain laminar flow under the prevailing conditions of stream turbulence and surface finish. A suction velocity ratio of approximately 0·0010 has proved necessary in order to ensure the preservation of laminar flow with the conditions prevailing in the wind-tunnel at Cambridge, although a lower figure may be adequate under the steadier air conditions of free flight.

As far as turbulent flow is concerned, it has been shown that distributed suction provides an effective method of thinning a turbulent boundary layer. Some evidence has also been accumulated to show that an asymptotic turbulent suction profile may be closely approached at sufficient values of suction velocity. A theoretical basis has been suggested for this type of boundary-layer flow, using the vorticity transfer theory, which has given good agreement with the experimental results.

1. *Introduction.*—Broadly speaking, there are three distinct objects which it may be possible to achieve, either separately or in combination, by the control of boundary-layer flow with distributed suction through a porous surface:—

(1) Preservation of laminar flow under conditions in which the flow would normally be turbulent, with consequent reduction of drag.

(2) Maintenance of flow without separation in the face of adverse pressure gradients, with possible reduction of form drag or increase of lift.

(3) Improvement of velocity distribution near a surface by thinning the boundary layer.

The present report is concerned with an experimental investigation of both laminar and turbulent boundary-layer flow along a flat plate with uniform distributed suction. The problem of flow against an adverse pressure gradient awaits further experimental study.

The great difference between the laminar and turbulent drag of a flat plate or thin streamlined body at large Reynolds numbers is well known. Attempts to reduce the drag of aircraft, by extending the region of laminar flow with the use of low-drag airfoil sections, have generally been disappointing. The necessary accuracy of construction, freedom from waviness, and high degree of surface finish have hitherto proved to be prohibitive under normal operating conditions. Distributed suction, however, appears to offer the possibility of preserving laminar flow with greatly enhanced stability at unlimited values of the Reynolds number. There are grave practical difficulties in the application of any effective form of suction to an aircraft, but the difficulties are primarily of a structural and mechanical nature and, with the exception of the problem of icing, the uncertainty as to whether or not the flow really will remain laminar under practical operating conditions may be largely removed. With uniform suction the boundary-layer velocity profiles should approach steadily towards the asymptotic exponential form[1]

$$\frac{u}{u_1} = 1 - e^{-v_s y/\nu} \quad \ldots \quad (1)$$

and stability calculations by Pretsch, Ulrich and others [2,3] suggest that, above a certain value of the ratio of suction velocity to stream velocity, complete stability against infinitesimal disturbances may be achieved for all Reynolds numbers. In Fig. 28, the effective total drag of a flat plate, with suction from the leading edge at the rate calculated by Ulrich for complete stability, is plotted against Reynolds number, together with the normal turbulent drag and the theoretical laminar drag without suction. The great reduction below the normal turbulent drag at high Reynolds numbers, which thus appears possible, is striking and the implications with regard to economy and range of transport aircraft are obvious.

The principal object of the present research was to undertake an experimental investigation of the engineering possibilities of this method of drag reduction, and to find out to what extent the drag figures implied by Ulrich's work could in fact be realised. In spite of the extent of the mathematical analysis applied to this problem by various investigators, there has been an almost complete lack of experimental investigation, and it was for this reason that the work at Cambridge University was originally undertaken.

Acknowledgments are due in the first place to Professor Sir Melvill Jones, under whose direction the work was carried out, and to Dr. J. H. Preston who gave advice throughout the investigation. Acknowledgments are also due to Mr. R. H. Bates and F/Lt. M. R. Head who assisted in taking readings during some of the experimental work, and to Mr. N. Surrey who constructed the necessary apparatus.

2. *Experimental Equipment.*—The experimental work which was carried out in the No. 2 Closed-Circuit Wind-Tunnel at Cambridge University consisted of a fairly extensive study of the boundary-layer flow over a flat plate with uniform suction and with zero pressure gradient in the direction of the undisturbed stream. The two principal experimental difficulties, encountered at the outset, were the construction of a flat porous surface and the accurate measurement of the boundary-layer velocity profiles.

The arrangement in the working-section of the wind-tunnel is shewn by the diagram in Fig. 1. The tunnel boundary layer was removed by means of a diffuser-shaped duct. The flat plate consisted of a short non-porous entry length followed by the porous surface. Various materials were tried, but the most satisfactory surface was one constructed from sheets of sintered bronze soldered together and supported on a steel grill. The porous surface formed the top of a suction chamber, which was connected to two small electrically-driven suction pumps. The flow of air through the surface could be measured by means of venturi meters connected in the pipe lines between the suction chamber and the pumps.

Measurements of the boundary-layer velocity profiles, at various points along the plate, were made by means of an exploring pitot-tube. The exploring pitot-tube was designed so that it could be located relative to the surface with an accuracy of $\pm$ 0·001 in. This was achieved by using a standard micrometer head for the feed, and by mounting this micrometer head on a vertical steel support held permanently in contact with the surface. The steel support was, in turn, held by a spring mounting in a streamlined cross-member spanning the working-section at a height of about 6 in. above the tunnel floor and fixed to the walls on either side. Any vibration or movement of the tunnel floor relative to the walls merely resulted in a movement of the vertical supporting member relative to the horizontal cross-beam. The pitot-tube was moved vertically relative to the tunnel floor by means of a flexible drive connected to the micrometer screw through a worm gear. The movement was effected manually from outside the tunnel but the micrometer reading was observed through a window in the tunnel wall. In this way, error due to backlash was eliminated. The pitot-tube itself was of fine bore and had a slightly flattened end. When the tube was in contact with the floor the effective centre was estimated to be 0·013 in. above the surface, and this estimate was confirmed by measurement of laminar Blasius profiles whose exact shape could be calculated.

The arrangement of the flat plate with a short non-porous entry length was chosen for experimental convenience. In the preliminary experiments an entry length of 6 in. was employed, but this was subsequently reduced to 4 in. and at the same time great care was taken to ensure a well-shaped leading edge and a smooth junction between the non-porous and porous sections of the surface. It was found that it was essential to prevent any disturbance from being set up in the boundary layer near the leading edge if transition was to be avoided further down the plate. A disturbance introduced at a point on the porous surface is not so critical since in this case the stabilising effect of the suction is immediately operative and can prevent transition. But a disturbance introduced *ahead* of the porous surface may be magnified sufficiently in the uncontrolled entry length so that the boundary layer is in a state of transition by the start of the porous surface, and in these circumstances suction will not succeed in restoring laminar flow. (*See* sections 3 and 4).

Tests were made to examine the uniformity of the porosity, and measurements of the local rate of flow through the surface indicated that the extreme variation of suction velocity was less than 10 per cent of the mean suction velocity. Over the central portion of the surface, where the observations of the boundary-layer profiles were actually made, the variation of suction velocity was in fact much less than this.

3. *Development of the Boundary-layer Velocity Profiles with Distance along the Plate.*—Preliminary experiments established the interesting and important result that if the boundary layer at the start of the porous section of the surface is already in a state of transition, no amount of suction can prevent the boundary-layer flow from becoming fully turbulent.

If transition is to be prevented by means of suction, it is essential that the suction should start in a region where the boundary layer is still in an undisturbed laminar condition. The safest arrangement would be to start the suction at the leading edge. This might indeed be the arrangement employed in practice in the case of an aerofoil, but for a flat plate with sharp leading edge there are obvious difficulties. As described in section 2, the experimental measurements were taken on a flat plate having a short non-porous entry length, but by careful construction it was possible to ensure that the boundary-layer profile at the start of the porous surface was of the undisturbed Blasius form.

Measurements of the boundary-layer velocity profiles were made at suitable intervals over the entire length of the porous surface using a constant rate of suction. The experimental profiles are reproduced in Figs. 2 to 10. The ratio of suction velocity to free-stream velocity for this series of tests was 0·0029, and the tunnel speed was approximately 57 ft/sec.

It will be observed that at the start of the porous section of the surface (x = 4·25 in.) a profile is obtained which fits very closely to the theoretical laminar Blasius profile. Without suction, transition appears to start fairly soon after the beginning of the porous surface. This is probably due to the fact that with the present form of construction (using 6 × 12-in. sheets of sintered bronze joined together to form a continuous plate) it is impossible to secure a really flat surface owing to the occurrence of slight ridges at the joints, but it may also be due to turbulence of the tunnel stream in the neighbourhood of the walls. A typical set of transition profiles is obtained for the case without suction, as shewn by the dotted curves in Figs. 4 to 10. At the end of the plate the velocity profile without suction has the appearance of a fully developed turbulent layer.

With suction applied, the velocity profiles approach rapidly towards the laminar asymptotic exponential form

$$\frac{u}{u_1} \doteq 1 - e^{-v_s y/\nu} \quad \ldots \quad (1)$$

as the distance x along the plate increases. This process is revealed clearly in Figs. 11 and 12 where the displacement thickness δ^* and the momentum thickness θ are plotted against distance x. From $x = 8$ in. onwards, the momentum thickness remains substantially constant and is in close agreement with the theoretical asymptotic value $\nu/2v_s$. The displacement thickness settles down in a similar manner to the theoretical asymptotic value ν/v_s. There is some slight variation from point to point along the plate, but this is simply due to local variation in the porosity of the surface. For example, at the point corresponding to the velocity profile of Fig. 9 the porosity is below standard but further on as in Fig. 11 the surface is better and the profile is in closer agreement with the asymptotic form.

4. *Effect of Stream Turbulence and Surface Disturbances on the Boundary Layer.*—In order to investigate the effect of stream turbulence the velocity profile was measured at the end of the plate with the same rate of suction but with different tunnel speeds. Results for tunnel speeds of 36, 61, and 95 ft/sec are shewn in Figs. 13 to 15. At the two lower speeds the velocity profiles are practically identical and in good agreement with the laminar exponential form. At the highest speed, however, the profile is entirely different and has a typically turbulent shape. It would appear that the unsteadiness of the tunnel stream, when running at maximum velocity, is responsible for transition in this case. This question of stream turbulence could be investigated further with the help of hot-wire apparatus. In the centre of the working-section the turbulence is quite low (of the order of 0·45 per cent) but it may be much greater close to the tunnel walls and floor. It would be of interest to carry out experiments with a flat plate mounted in the centre of the tunnel, but flight experiments would appear to offer the only sure way of eliminating the doubtful effects of stream turbulence altogether.

To investigate the effect of surface disturbances, measurements were made of the profile at the end of the plate with a wire stretched across the surface at a point approximately 18 in. upstream (*i.e.*, 6 in. downstream from the start of suction). The results of these experiments for various sizes of wire are shewn in Figs. 16 to 18. It will be observed that a wire of 0·0045-in. diameter in contact with the surface has very little effect on the velocity profile downstream, but it must be emphasised that a disturbance of this nature can be successfully surmounted only if it occurs in a region where the asymptotic laminar profile is already well established. With a larger diameter wire, a typical turbulent suction profile is observed at the end of the plate. It might be possible, however, to deal successfully with these larger disturbances by employing a higher suction velocity. The ratio of suction velocity to stream velocity employed in the above experiments was 0·0028, which is approximately 24 times Ulrich's figure for the minimum rate above which all infinitesimal disturbances should be damped.

The effect of a fine wire stretched across the leading edge of the plate ahead of the start of suction was to produce turbulent suction flow downstream, even at the highest available rates of suction. The general conclusion, therefore, is that the laminar exponential suction profile can be established and retained only if the boundary layer is in an undisturbed laminar condition can be established and retained only if the boundary layer is in an undisturbed laminar condition at the start of the suction region. But once the laminar suction profile has been established, it is able to surmount small disturbances which would normally be sufficient to promote transition.

5. *Variation of Total Drag with Suction Velocity*.—The total effective drag of a flat plate with uniform suction consists of two parts—the momentum drag and the ideal equivalent pump drag (*see* Appendix I). Experiments were made in order to determine this total effective drag by measuring the velocity profiles of the boundary layer at the downstream end of the plate at various rates of suction. These experiments were carried out with a tunnel speed of 53 ft/sec while the ratio of suction velocity to stream velocity was varied from zero to 0·0032. The momentum drag was determined from the measured velocity profiles. The equivalent pump drag was calculated from the known rates of suction.

Measured velocity profiles are plotted in Figs. 19 to 23 with the ratio of suction velocity to free-stream velocity varying from zero in Fig. 19 to 0·00318 in Fig. 23. The asymptotic exponential profile appropriate to each suction velocity is also plotted, but only in the case of Figs. 22 and 23 is the suction velocity ratio sufficiently great for the boundary layer to approach closely to asymptotic conditions by the end of the plate. With zero suction the boundary layer has a typically turbulent velocity profile at the end of the plate, owing to the fact that in the absence of suction transition begins a short way downstream from the start of the porous surface. With very low suction velocities the flow in the boundary layer appeared to be unsteady, and the velocity ratio of Fig. 20, $v_s/u_1 = 0 \cdot 0008$, was about the lowest at which consistent measurements could be taken. With higher suction velocity ratios the flow was quite steady and evidently laminar. The velocity profiles of Figs. 20 to 23 are plotted together, for purposes of comparison, in Fig. 24.

The momentum thickness of the boundary layer θ, computed from the measured velocity profiles, is plotted against suction velocity ratio in Fig. 25. The corresponding momentum and total-drag coefficients are plotted in Fig. 26. Also plotted on Fig. 26 is the theoretical total drag coefficient calculated on the assumption of laminar flow at all suction velocities (*see* Appendix I). At the higher suction velocities the experimental points are in very close agreement with the theoretical value, but at the lower suction velocities the experimental curve diverges from the theoretical one owing to the fact that with zero suction the flow is turbulent over the greater part of the plate. The net result is that a minimum total drag is obtained at approximately the lowest suction velocity ratio at which laminar flow can survive.

It will be seen from Fig. 26 that the maximum total drag reduction obtained in these experiments is about 25 per cent. At first sight this may not appear to be very startling. However, at the Reynolds number of these experiments, the maximum possible drag reduction is only from 0·00251 (the measured value without suction) to 0·00150 (the Blasius value for laminar flow), *i.e.*, about a 40 per cent reduction. At higher Reynolds numbers the difference between the laminar and turbulent drag coefficients is, of course, much larger, and the possible saving to be derived from suction is correspondingly greater.

It is shewn in Appendix I that the total equivalent drag coefficient for a flat plate with suction, starting from the leading edge, assuming no pressure drop through the surface, zero duct losses, and 100 per cent pump efficiency, is given by—

$$C_D = \frac{v_s}{u_1}\left[\frac{1}{\xi_L}\frac{\theta}{\theta_s} + 1\right] \qquad \text{(2)}$$

where $$\xi_L = \left(\frac{v_s}{u_1}\right)^2 \frac{u_1 L}{\nu}$$

and L length of plate

θ momentum thickness at trailing edge

θ_s asymptotic momentum thickness

$= \nu/2v_s$

In Fig. 27 curves of C_D against v_s/u_1 are plotted for values of $R_L = u_1L/\nu$ of 10^6, 10^7, and 10^8 using the appropriate values of θ/θ_s. These curves, however, are ideal in the sense that they assume laminar flow down to zero suction velocity and include no allowance for losses in the suction system. In practice, with turbulent flow at zero suction, the curves of C_D would show a definite minimum at some particular value of v_s/u_1. The question of this optimum suction velocity ratio is discussed in the following section.

6. *The Optimum Rate of Suction.*—For the case of the flat plate, if the flow in the boundary layer could be relied on to remain laminar under all circumstances, the optimum rate of suction would be zero. This is immediately apparent from Fig. 26. In general, however, the flow in the boundary layer will be at least partly turbulent in the absence of suction owing to imperfections in the flatness of the surface or to turbulence in the external air stream. The value of suction, as far as flat plate drag is concerned, lies in the preservation of laminar flow in circumstances when the boundary layer, if left to its own devices, would become turbulent.

The optimum rate of suction, then, is the minimum rate which is sufficient to maintain laminar flow with a given degree of surface finish and with the prevailing stream turbulence.

Ulrich has investigated the problem of the stability of flow in the inlet region with uniform suction[3], and reaches the conclusion that if the ratio of suction velocity to stream velocity is greater than 0·000118 the boundary-layer flow should be entirely stable in face of infinitesimal disturbances. The experimental results described in this report suggest that in practice a somewhat higher suction ratio may be required. For the plate with non-porous entry length, on which the experiments were made, the necessary suction velocity ratio was found to be about 0·0008, *i.e.*, about 7 times Ulrich's figure. However, the comparison is not entirely fair because of the non-porous entry length.

To give some idea of the possible range of drag coefficient obtainable, the total-drag coefficient is plotted in Fig. 28 for the case of a flat plate with suction starting from the leading edge. Curves are drawn for three different suction velocity ratios. The lowest is for Ulrich's figure of 0·000118 and represents the ultimate goal. The other two curves are for suction velocity ratios of 0·0005 and 0·0010 respectively. The experiments have shown that with the higher of these two figures there is no difficulty in securing laminar flow. A lower figure may well suffice if suction starts from the leading edge, and also in free flight where the stream turbulence may be negligible. The ratio of 0·0010 can be regarded as a safe—and in fact a rather conservative—figure.

The important point is that, even with the suction velocity ratio of 0·0010, a quite spectacular reduction of drag below the normal turbulent figure is possible at high Reynolds numbers. For instance, at a Reynolds number of 10^7 the flat plate drag coefficient for turbulent flow is about 0·003. The total drag with suction at the same Reynolds number and with $v_s/u_1 = 0{\cdot}0010$ would be 0·0011, *i.e.*, about one-third of the normal turbulent drag. With $v_s/u_1 = 0{\cdot}0005$ the total drag would be 0·0007, and with Ulrich's figure of 0·000118 for v_s/u_1 the total-drag coefficient would be down to 0·00046 which is about 15 per cent of the turbulent drag without suction.

These conclusions must, however, be qualified by consideration of the various losses which may arise in the suction system. There are three distinct sources of departure from ideal conditions—pressure drop through the surface, ducting losses, and pump or compressor efficiency.

If there is a pressure drop Δp through the surface, additional power is required for the suction pump, and the total equivalent drag coefficient for a flat plate with suction extending over the whole surface becomes

$$C_D = \frac{v_s}{u_1}\left[\frac{1}{\xi_L}\frac{\theta}{\theta_s} + 1 + \frac{\Delta p}{\frac{1}{2}\rho u_1^2}\right] \quad \ldots \quad (3)$$

using the same notation as before.

For the case of a flat plate, or for a *portion* of the surface of an airfoil over which the external pressure remains substantially constant, there would be no difficulty in keeping the pressure drop Δp down to a very low value indeed by using a sufficiently porous surface such as a very fine phospor-bronze wire gauze. However, in most practical applications of suction, it will be necessary to cater for a variable external pressure distribution, as for instance in the case of an airfoil where the pressure distribution changes with incidence. In such applications there are two alternatives. The first is to use a highly porous material but to divide the surface up into a large number of regions each with its own suction chamber operating at a pressure only slightly less than the external pressure over the region concerned. This would involve the serious practical difficulty of drawing air from a large number of suction chambers each at a different pressure. The second alternative is to use a single suction chamber but with a material such that the pressure drop Δp is at least as great as the maximum external pressure difference occurring over the suction area. To ensure a *uniform* rate of suction, the pressure drop Δp would naturally have to be large compared with the maximum external pressure difference. However, there is no particular objection to having a suction velocity which varies from point to point along the surface with the external pressure. The normal procedure, therefore, would be to design the surface so that the pressure drop Δp is equal to, or slightly greater than, the maximum external pressure difference. In general this means that Δp would have to be of the same order of magnitude as $\frac{1}{2}\rho u_1^2$ and it follows, by comparison of equations (2) and (3), that the total equivalent drag coefficient might in practice be increased by a quantity approximately equal to v_s/u_1.

7. *Turbulent Flow with Suction.*—It has already been stated that the principal object of porous suction is the preservation of laminar flow under conditions where the flow would otherwise be turbulent. It may seem strange, therefore, to trouble about turbulent flow with suction. However, there are three good reasons for doing so. In the first place it is as well to know, in any practical application of suction, just what will happen if disturbances are introduced which are sufficiently large to overcome the stabilizing effect of the suction. Secondly, there are a number of possible applications of suction where the flow would necessarily be turbulent. In such cases, as for instance in the passages of hydraulic turbo-machinery, axial compressors, and ducting, etc., suction might be used simply to improve a velocity distribution or to keep a boundary layer reasonably thin. It is true that in most applications of this type there will be adverse pressure gradients to be coped with as well. However, it is useful as a starting point to have some reliable information about the simple case of flow with zero pressure gradient. Finally, it was thought worth while to make some observations of turbulent flow with suction simply for the sake of accumulating some fresh information about turbulent boundary-layer flow.

8. *Theoretical Considerations in Turbulent Flow.*—The momentum equation for boundary-layer flow with uniform suction and zero pressure gradient takes the same form whether the flow is laminar or turbulent

$$\frac{\tau_0}{\rho U_1^2} = \frac{\partial \theta}{\partial x} + \frac{v_s}{U_1} \quad \ldots \quad (4)$$

where τ_0 is the shearing stress at the wall.

It is not by any means obvious that, with uniform suction, an asymptotic profile will be attained with turbulent flow. To decide this point, an appeal must be made to experiment. However, if asymptotic conditions are in fact realised, $\partial\theta/\partial x = 0$ and therefore

$$\frac{\tau_0}{\rho U_1^2} = \frac{v_s}{U_1} \qquad \ldots \qquad (5)$$

i.e., the shearing stress at the wall will have the same value as under laminar asymptotic conditions.

In terms of the mean velocity components U, V, the equation of motion for a turbulent boundary layer is—

$$U\frac{\partial U}{\partial x} + V\frac{\partial U}{\partial y} = \nu\frac{\partial^2 U}{\partial y^2} + \frac{1}{\rho}\frac{\partial \tau}{\partial y} \qquad \ldots \qquad (6)$$

(where τ is the *turbulent* shear stress) and the equation of continuity is—

$$\frac{\partial U}{\partial x} + \frac{\partial V}{\partial y} = 0. \qquad \ldots \qquad (7)$$

Under asymptotic conditions, $\partial U/\partial x = 0$ and, with uniform suction, V = const. = $-v_s$, therefore, the equation of motion for asymptotic condition is

$$-v_s\frac{dU}{dy} = \nu\frac{d^2U}{dy^2} + \frac{1}{\rho}\frac{d\tau}{dy}. \qquad \ldots \qquad (8)$$

Close to the surface in the laminar sub-layer the turbulent stress term may be neglected, *cf.* the viscous term, so that from $y = 0$ to $y = \varepsilon$ (say) we can assume—

$$-v_s\frac{dU}{dy} = \nu\frac{d^2U}{dy^2}. \qquad \ldots \qquad (9)$$

But beyond the laminar region, the viscous term may be neglected, *cf.* the turbulent stress term, so that from $y = \varepsilon$ to $y = \delta$

$$-v_s\frac{dU}{dy} = \frac{1}{\rho}\frac{d\tau}{dy}. \qquad \ldots \qquad (10)$$

In the region near $y = \varepsilon$, *i.e.*, at the edge of the laminar sub-layer, the viscous and turbulent stress terms are of the same order of magnitude, so that neither equation (9) nor (10) can represent the true state of affairs. However, for a first approximation it is reasonable to divide the flow into two distinct regions in the manner assumed.

On the basis of mixture length theory there are two alternative forms for the turbulent shear stress τ. On Prandtl's momentum transfer theory

$$\tau = \rho L^2\left(\frac{dU}{dy}\right)^2 \qquad \ldots \qquad (11)$$

and on Taylor's vorticity transfer theory

$$\frac{\partial \tau}{\partial y} = \rho L^2\frac{dU}{dy}\frac{d^2U}{dy^2}. \qquad \ldots \qquad (12)$$

For the mixing length L we can assume either

$$L = ky \quad \ldots \quad (13)$$

as in the theory of flow in pipes, k being a constant,

or $$L = ky\left(1 - \frac{y}{2\delta}\right) \quad \ldots \quad (14)$$

which is an extension of assumption (13) allowing for the fact that L cannot increase indefinitely with y,

or $$L = \frac{k\,(dU/dy)}{d^2U/dy^2} \quad \ldots \quad (15)$$

as in Kármán's similarity theory. The use of either equation (11) or (12) in equation (10), together with assumption (13), (14) or (15) for the mixing length, will result, after integration between appropriate boundary conditions, in a velocity profile for the outer or turbulent part of the boundary layer.

It was found that agreement could be obtained with the form of the experimentally determined velocity profiles only by using the vorticity transfer theory (12), together with assumption (13) or (15) for the mixing length.

From equations (10), (12), and (15)*,

$$-v_s = \frac{k^2\,(dU/dy)^2}{d^2U/dy^2}$$

or $$\frac{d^2U/dy^2}{(dU/dy)^2} = -\frac{k^2}{v_s}.$$

Therefore, integrating, $-\dfrac{1}{dU/dy} = -\dfrac{k^2}{v_s}y + c$

the constant c is assumed to be zero, implying that if the turbulent profile is extended down to the surface, $dU/dy \to \infty$ as $y \to 0$, as with other turbulent velocity profiles.

Therefore $$dU = \frac{v_s}{k^2}\frac{dy}{y}$$

or $$\int_U^{U_1} dU = \frac{v_s}{k^2}\int_y^{\delta}\frac{dy}{y}.$$

Therefore $$(U_1 - U) = \frac{v_s}{k^2}\log_e\frac{\delta}{y} = -\frac{v_s}{k^2}\log_e\frac{y}{\delta}.$$

Therefore $$1 - \frac{U}{U_1} = -\frac{1}{k^2}\frac{v_s}{U_1}\log_e\frac{y}{\delta}. \quad \ldots \quad (16)$$

Therefore, from $y = \varepsilon$ to $y = \delta$ the velocity profile should have the form

$$\frac{U}{U_1} = 1 + \frac{1}{k^2}\frac{v_s}{U_1}\log_e\frac{y}{\delta}. \quad \ldots \quad (17)$$

This result can easily be checked by plotting the experimental values of $1 - U/U_1$ against $\log_e y$.

* The use of assumption (13) is discussed in Appendix II. The final result is the same as with assumption (15).

The artificial division into two distinct regions of flow, represented by the differential equations (9) and (10), therefore yields the following results for the form of the velocity profile— In the *laminar* region, $y = 0$ to $y = \varepsilon$, from equation (9)

$$\left.\begin{aligned} U &= U_1\left(1 - e^{-v_s y/\nu}\right) \\ \frac{dU}{dy} &= U_1 \frac{v_s}{\nu} e^{-v_s y/\nu} \\ \frac{d^2U}{dy^2} &= -U_1 \frac{v_s^2}{\nu^2} e^{-v_s y/\nu} \end{aligned}\right\} \qquad \ldots \quad (18)$$

and the viscous stress at the wall satisfies condition (5). In the *turbulent* region $y = \varepsilon$ to $y = \delta$, from equation (10)

$$\left.\begin{aligned} U &= U_1\left(1 + \frac{1}{k^2}\frac{v_s}{U_1}\log_e \frac{y}{\delta}\right) \\ \frac{dU}{dy} &= \frac{1}{k^2}\frac{v_s}{y} \\ \frac{d^2U}{dy^2} &= -\frac{1}{k^2}\frac{v_s}{y^2} \end{aligned}\right\} \qquad \ldots \quad (19)$$

At $y = \varepsilon$ we must have $U_{\text{lam.}} = U_{\text{turb.}}$, therefore, from equations (18) and (19) ε must be related to the boundary-layer thickness by

$$e^{-v_s y/\nu} = -\frac{1}{k^2}\frac{v_s}{U_1}\log_e \varepsilon/\delta. \qquad \ldots \quad (20)$$

It is not possible, however, to satisfy the condition of continuity in dU/dy at $y = \varepsilon$ owing to the artificial nature of the division into two regions.

If one follows the turbulent velocity profile equation (17) in towards the surface, one would expect a steady divergence from the experimental velocity profile as the viscous stress term, which is neglected in equation (10), becomes comparable with the turbulent stress term. If equation (17) continued to apply, the two terms would become *equal* when

$$\nu \frac{d^2U}{dy^2} = L^2 \frac{dU}{dy}\frac{d^2U}{dy^2} = \frac{k^2(dU/dy)^3}{d^2U/dy^2}$$

or, from equation (19) $y = \dfrac{\nu}{v_s}$ .. .. (21)

this value of y is the same as the displacement thickness of the *laminar* asymptotic profile, and it gives an indication of the thickness of the laminar sub-layer in the case of turbulent flow.

9. *Experimental Results with Turbulent Flow.*—Two sets of experiments have been carried out in the No. 2 Closed-Circuit Wind-Tunnel. In the first set of experiments, conditions were such that at the start of the porous section of the surface the boundary layer was just on the point of transition. The process of transition from laminar to turbulent flow took place over the first few inches of the porous surface, and by the downstream end the boundary layer was apparently fully turbulent both with and without suction. Measurements of the velocity profiles were made at suitable intervals along the length of the plate. Two such profiles, taken near the downstream end at $x = 25 \cdot 8$ and $x = 29 \cdot 5$ in. respectively, are reproduced in Figs. 29 30. These results provide definite evidence that an asymptotic profile can be attained with turbulent flow.

The profiles of Figs. 29, 30 are re-plotted on Fig. 31 in the form of $(1 - U/U_1)$ against $\log_e y$. The measured points for the two suction profiles lie fairly well together on a single straight line, within the limits of experimental error, in agreement with equation (17). The only serious departure from the straight line occurs close to the wall, where the turbulent profile merges into the laminar sub-layer. Also plotted on Fig. 31 are the results without suction for $x = 25 \cdot 8$ and $29 \cdot 5$ in. These indicate, not only the normal steady growth in the thickness of the boundary layer without suction, but also the fact that the form of the velocity distribution is entirely different from the case with suction.

The numerical value of the quantity $(1/k^2)$ (v_s/U_1) measured by the slope of the line in Fig. 31 is $0 \cdot 055$, and since in this case $v_s/U_1 = 0 \cdot 0030$ the appropriate value for the constant k appears to be $0 \cdot 233$. If, however, the turbulent profile has not quite reached its final asymptotic form, *i.e.*, if there is still a very slow growth in the boundary-layer thickness, the correct value for asymptotic conditions may be slightly higher. Even so, it appears to be considerably less than the value $0 \cdot 36$ which is usually assumed for the Kármán similarity theory for turbulent flow in pipes. The experimental value for the boundary-layer thickness δ from Fig. 31 is $0 \cdot 270$ in. Using this value, the laminar and turbulent parts of the profile corresponding to equations (18) and (19) are plotted in Fig. 32 together with a set of experimental points with suction. The general form of the turbulent suction profile can thus be accounted for.

In Fig. 32 the junction between the laminar and turbulent portions of the calculated profile occurs at $0 \cdot 021$ in., *i.e.*, $\varepsilon = 0 \cdot 021$ in. and this is very nearly equal to twice the displacement thickness of the *laminar* asymptotic profile. This result is in good qualitative agreement with the considerations leading up to equation (21) above.

In a later set of experiments, conditions were such that the flow was normally laminar over the entire surface of the plate provided suction was applied at a rate greater than $v_s/U_1 = 0 \cdot 0010$. In this case turbulent flow was established over the whole length of the plate by fixing a wire of $0 \cdot 005$-in. diameter across the plate at the leading edge. A relatively small disturbance of this nature will result in turbulent flow with suction provided it is introduced *ahead* of the start of the suction region, *i.e.*, provided the boundary layer is already either turbulent or in a state of transition at the start of the porous surface. A small disturbance will not produce turbulent conditions if it is introduced in a region where laminar asymptotic suction flow is well established and the rate of suction is high enough.

The results of two measurements at different rates of suction are reproduced in Figs. 33, 34 for both laminar and turbulent flow. In Fig. 33 $v_s/U_1 = 0 \cdot 00149$ and it will be observed that asymptotic conditions have not yet been reached at this relatively low rate of suction, either under laminar or turbulent conditions. (This conclusion is supported by other measurements of the boundary-layer profiles taken at intervals along the plate). In Fig. 34, however, with $v_s/U_1 = 0 \cdot 00332$, asymptotic conditions appear to be well established. The turbulent profile of Fig. 34 is re-plotted on Fig. 35 in the form of $(1 - U/U_1)$ against $\log_e y$, and the result is again a straight line. The slope in this case is $0 \cdot 066$, and with $v_s/U_1 = 0 \cdot 00332$, this gives $k = 0 \cdot 225$ which is in very good agreement with the previous result.

Taking the experimental value of $\delta = 0 \cdot 333$ in. from Fig. 35, the laminar and turbulent portions of the asymptotic turbulent profile are plotted on Fig. 36, together with the experimental points. The junction in this case occurs at $y = 0 \cdot 025$ in., *i.e.*, $\varepsilon = 0 \cdot 025$ in. and this value is equal to about $1 \cdot 8$ times the displacement thickness of the *laminar* asymptotic profile.

10. *Prediction of the Boundary-layer Thickness with Turbulent Flow.*—In the calculations given above, appeal has been made to experiment for the value of the constant k and the boundary-layer thickness δ. However, an estimate can be made of the value of δ in any particular case in the following manner. It has been shewn that an appreciable divergence must be expected between the actual velocity profile and the turbulent profile of equation (17) for values of y less than ν/v_s, owing to the relative magnitude of the turbulent and viscous stress terms. It is reasonable to argue, therefore, that the artificial junction between the laminar and turbulent

regions should occur at a somewhat larger value of y, but bearing a definite ratio to the quantity ν/v_s. The experiments have suggested that this ratio is in the neighbourhood of 1·8 or 1·9. If we assume that $\varepsilon = 1{\cdot}9\ \nu/v_s$, it follows from equation (20) that

$$-\frac{1}{k^2}\frac{v_s}{U_1}\log_e\frac{\varepsilon}{\delta} = e^{-1\cdot 9} = 0\cdot 1495.$$

Therefore, if $k = 0{\cdot}23$, $\dfrac{\delta}{\varepsilon} = \exp\dfrac{0\cdot 0079}{v_s/U_1}$

or
$$\frac{\delta v_s}{\nu} = 1\cdot 9\exp\frac{0\cdot 0079}{v_s/U_1}. \qquad (22)$$

The quantity $\delta v_s/\nu$ is plotted against v_s/U_1 in Fig. 37*. However, this result requires further experimental confirmation, at least in regard to the precise values of the constant k and the factor $\varepsilon\ v_s/\nu$.

It has thus been possible, on the basis of the vorticity transfer theory, to account for the general form of the mean velocity distribution in a turbulent boundary layer with uniform suction. The velocity distribution in the outer or turbulent portion of the boundary layer is represented by equation (17).

A similar method of calculation based on the momentum transfer theory, however, yields a result which is not in accordance with the experimental measurements (*see* Appendix III). In view of the doubtful validity of mixture length theory there may not be any great significance in this comparison, nevertheless it is of some interest because of the fact that asymptotic flow with suction is the only case of turbulent boundary-layer flow where similarity of velocity profiles can be assured.

One useful experimental result has been established,—that distributed suction provides a very effective method of thinning a turbulent boundary layer. Further investigation is required on the subject of turbulent boundary-layer flow with suction against an adverse pressure gradient.

REFERENCES

No.	*Author*	*Title, etc.*
1	J. H. Preston	The Boundary Layer Flow over a Permeable Surface through which Suction is Applied. R. & M. 2244. February, 1946.
2	J. Pretsch	Transition Start and Suction. *Jahrbuch d. Deutschen Luftfahrtforschung.* 1942. A.R.C. 10,291. (Unpublished).
3	W. Ulrich	Theoretical Investigation of Drag Reduction in Maintaining the Laminar Boundary Layer by Suction. N.A.C.A. Tech. Memo. No. 1121.
4	S. Goldstein	Low Drag and Suction Airfoils. *Journal of Aero. Sciences.* April 1948.
5	A. A. Griffith and F. W. Meredith..	Possible Improvement in Aircraft Performance due to use of Boundary-layer Suction. A.R.C. 2315.
6	H. Schlichting	The Boundary Layer of a Flat Plate under Conditions of Suction and Air Ejection. A.R.C. 6634, R.T.P. Trans. 1753. (Unpublished.)
7	B. Thwaites	On the Flow Past a Flat Plate with Uniform Suction. R. & M. 2481. February, 1946.
8	Iglisch	Report No. 43/22. Aerodynamisches Insitut der T.H. Braunschweig.

* It is important to note that at very low values of the ratio v_s/U_1 the approach towards asymptotic conditions may be very slow. In such circumstances the asymptotic value of the boundary-layer thickness given by equation (22) will not generally be realised in practice.

LIST OF SYMBOLS

x	Distance parallel to surface
y	Distance perpendicular to surface
u	Velocity component in x-direction (laminar flow)
v	Velocity component in y-direction (laminar flow)
U	Mean velocity component in x-direction (turbulent flow)
V	Mean velocity component in y-direction (turbulent flow)
u_1 or U_1	Velocity of undisturbed stream (outside boundary layer)
v_s	Suction velocity
τ	Shear stress
ρ	Fluid density
ν	Kinematic viscosity
δ^*	Displacement thickness
δ_s^*	Displacement thickness of asymptotic profile
θ	Momentum thickness
θ_s	Momentum thickness of asymptotic profile
δ	Thickness of turbulent boundary layer
ε	Distance from surface to the artificial boundary between laminar and turbulent regions of the boundary layer

APPENDIX I

Note on the Total Drag of a Flat Plate with Uniform Suction

Consider the case in which suction extends from $x = x_0$ to $x = l$ and let the length of the porous section of the surface be s, *i.e.*, $l - x_0 = s$.

Let the uniform suction velocity be v_s and the stream velocity u_1.

The total drag is made up of the momentum drag of the wake D_w and the drag equivalent D_p of the power P required to restore the total head of the sucked air.

$$D_w = \rho u_1^2 \int_0^\infty \frac{u}{u_1}\left(1 - \frac{u}{u_1}\right) dy = \rho u_1^2 \theta$$

where θ is the momentum thickness at the downstream end of the plate.

If asymptotic conditions are reached, $\frac{u}{u_1} = 1 - e^{-v_s y/\nu}$

and $$\theta = \theta_s = \int_0^\infty e^{-v_s y/\nu} \left(1 - e^{-v_s y/\nu}\right) dy = \frac{\nu}{2v_s} \cdot$$

In general, however, θ will differ in value from θ_s so that $\theta = (\nu/2v_s)\ (\theta/\theta_s)$.

For the case in which suction starts from the leading edge, the variation of θ/θ_s with $(v^s/u_1)^2\ (u_1 x/\nu)$ is known from Iglisch's exact solution for the inlet region. Preston has also given a good approximate solution.

The power required ideally (*i.e.*, with 100 per cent pump efficiency, no pressure drop through the surface, and zero duct losses) to step up the total head of the sucked air, per unit span, is given by $P = \rho s v_s\ (u_1^2/2) = \frac{1}{2}\rho u_1^3 s\ (v_s/u_1)$ the equivalent drag is $D_p = \frac{1}{2}\rho u_1^2 s\ (v_s/u_1)$.

Therefore, the total drag is

$$D = D_w + D_p = \tfrac{1}{2}\rho u_1^2 \left[\frac{\nu}{v_s}\frac{\theta}{\theta_s} + s\frac{v_s}{u_1}\right]$$

$$= \tfrac{1}{2}\rho u_1^2 l \left[\frac{\nu}{v_s l}\frac{\theta}{\theta_s} + \frac{s}{l}\frac{v_s}{u_1}\right].$$

Therefore $$C_D = \frac{v_s}{u_1}\left[\frac{u_1}{v_s}\frac{\nu}{v_s l} \cdot \frac{\theta}{\theta_s} + \frac{s}{l}\right].$$

Therefore $$C_D = \frac{v_s}{u_1}\left[\frac{1}{\xi} \cdot \frac{\theta}{\theta_s} + \frac{s}{l}\right] \text{ where } \xi_l = \left(\frac{v_s}{u_1}\right)^2 \frac{u_1 l}{\nu}$$

and if suction starts from the leading edge,

$$C_D = \frac{v_s}{u_1}\left[\frac{1}{\xi_l} \cdot \frac{\theta}{\theta_s} + 1\right].$$

In Fig. 27 curves of C_D against v_s/u_1 are plotted for values of $R_l (= u_1 l/\nu)$ of 10^6, 10^7, and 10^8, using the appropriate values of θ/θ_s taken from Iglisch's solution.

APPENDIX II

Derivation of the Form of the Turbulent Asymptotic Profile on the Basis of the Vorticity Transfer Theory, but with an Alternative Assumption for the Mixing Length.

If we assume that $L = ky$ as in the ordinary theory of turbulent flow in pipes, then from equations (10) and (12)

$$-v_s \frac{dU}{dy} = k^2 y^2 \frac{dU}{dy}\frac{d^2U}{dy^2}$$

or $$\frac{d^2U}{dy^2} = -\frac{v_s}{k^2 y^2} \ .$$

Therefore, integrating, $\frac{dU}{dy} = \frac{v_s}{k^2 y} + c$

assuming that $\frac{dU}{dy} \to 0$ as $y \to \infty$, the value of the constant must be zero.

Therefore $\int_U^{U_1} dU = \frac{v_s}{k^2} \int_y^{\delta} \frac{dy}{y}.$

Therefore $U_1 - U = -\frac{v_s}{k^2} \log_e \frac{y}{\delta}$

or $\frac{U}{U_1} = 1 + \frac{1}{k^2} \frac{v_s}{U_1} \log_e \frac{y}{\delta}.$

This is the same result as equation (17).

APPENDIX III

Turbulent Asymptotic Profile Calculated on the Basis of the Momentum Transfer Theory

From equations (10) and (11) $-v_s \frac{dU}{dy} = \frac{d}{dy}\left[L^2 \left(\frac{dU}{dy}\right)^2\right]$

Therefore, integrating, $-v_s U = L^2 \left(\frac{dU}{dy}\right)^2 + c$

and since $U \to U_1$ as $\frac{dU}{dy} \to 0$ $\qquad c = -v_s U_1$

Therefore $v_s(U_1 - U) = L^2 \left(\frac{dU}{dy}\right)^2.$

Using assumption (13) for the mixing length (as in Appendix II),

$$v_s(U_1 - U) = k^2 y^2 \left(\frac{dU}{dy}\right)^2.$$

Therefore $\frac{dU}{dy} = \frac{v_s^{1/2}}{ky} (U_1 - U)^{1/2}.$

Therefore $\frac{v_s^{1/2}}{k} \int_y \frac{dy}{y} = \int_U^{U_1} \frac{dU}{(U_1 - U)^{1/2}}.$

Therefore $\frac{v_s^{1/2}}{k} \log_e \frac{\delta}{y} = 2(U_1 - U)^{1/2}.$

Therefore $\left(1 - \frac{U}{U_1}\right)^{1/2} = -\left(\frac{v_s}{U_1}\right)^{1/2} \frac{1}{2k} \log_e \frac{y}{\delta}$

or $\frac{U}{U_1} = 1 - \frac{1}{4k^2} \frac{v_s}{U_1} \left[\log_e \frac{y}{\delta}\right]^2.$

According to the momentum transfer theory, therefore, a straight line should be obtained by plotting $(1 - U/U_1)^{1/2}$ against $\log_e y$. But this is not in accordance with the experimental results.

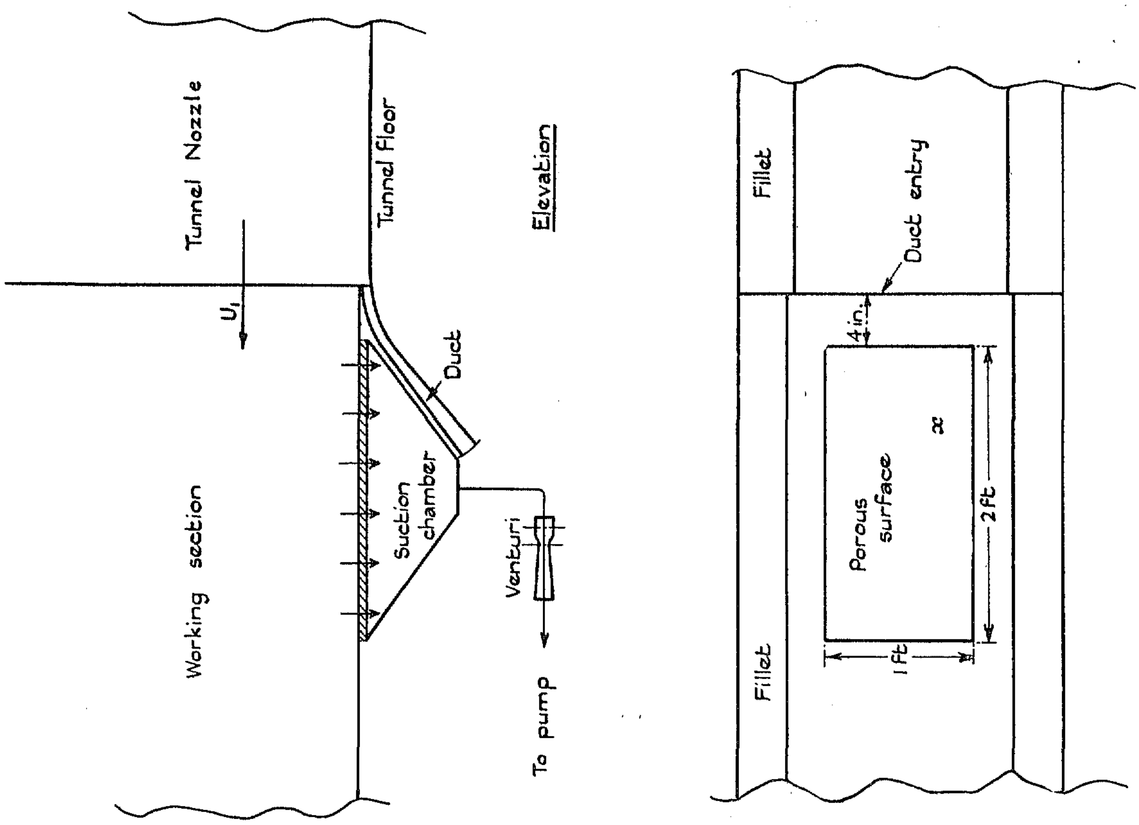

FIG. 1. Diagram of apparatus

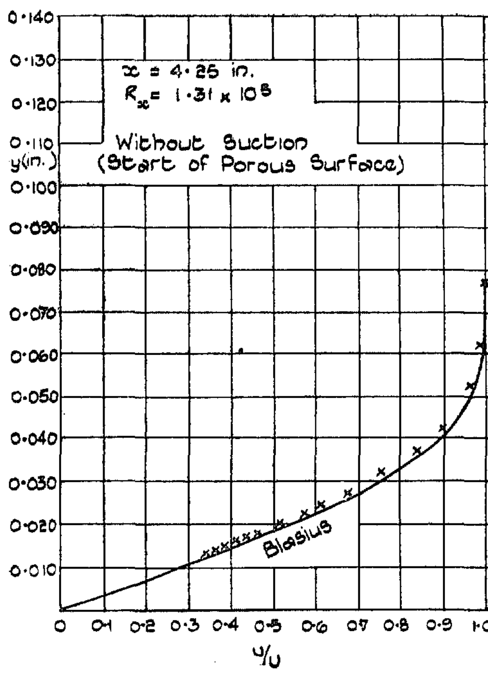

FIG. 2.

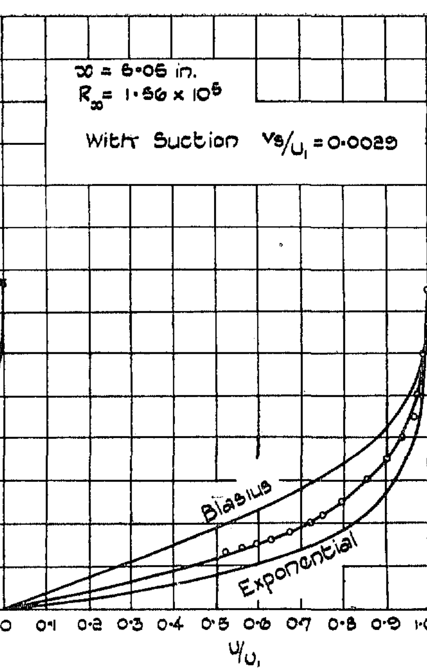

FIG. 3.

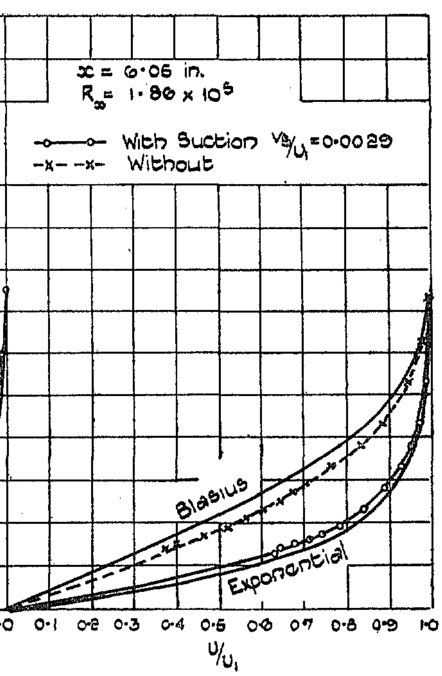

FIG. 4.

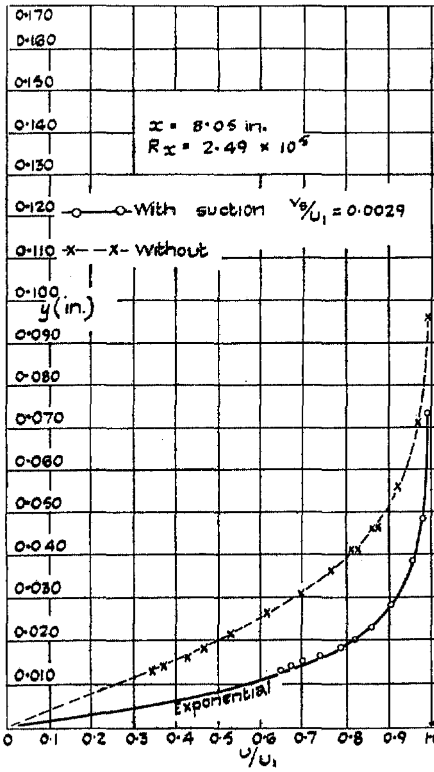

FIG. 5.

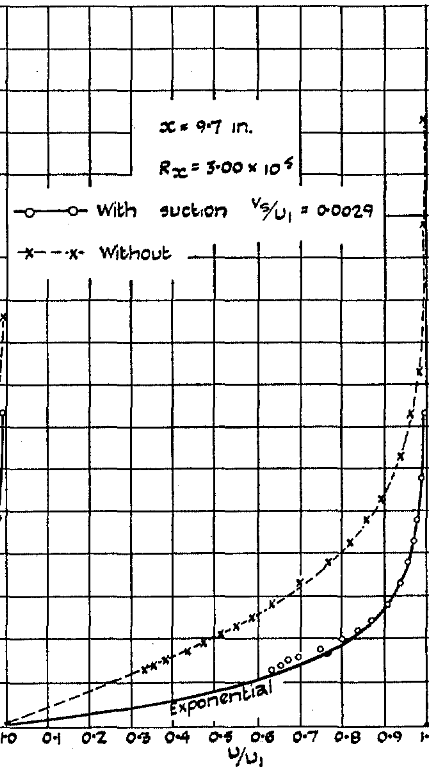

FIG. 6.

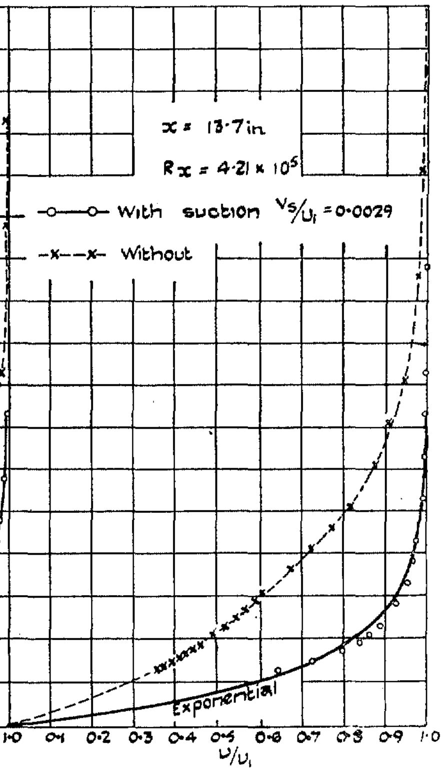

FIG. 7.

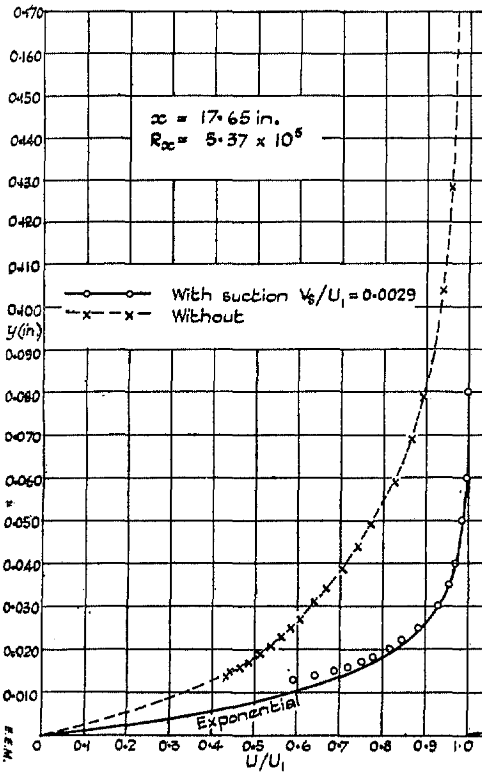

FIG. 8.

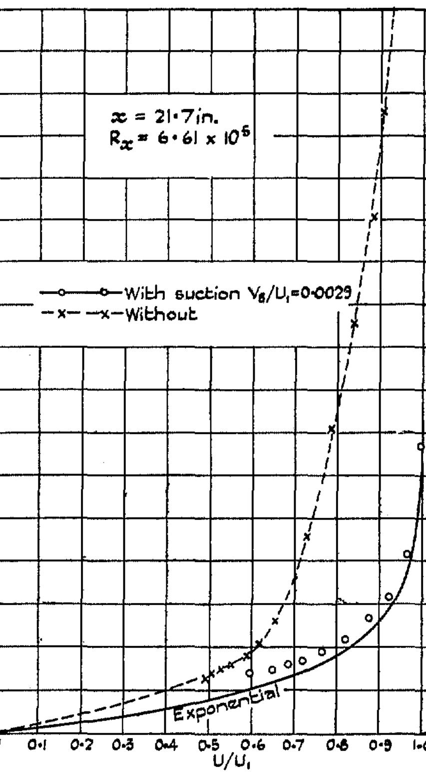

FIG. 9.

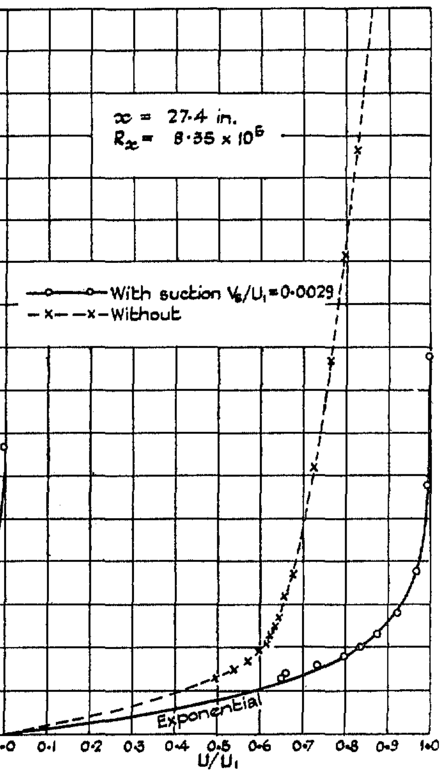

FIG. 10.

(22309) B

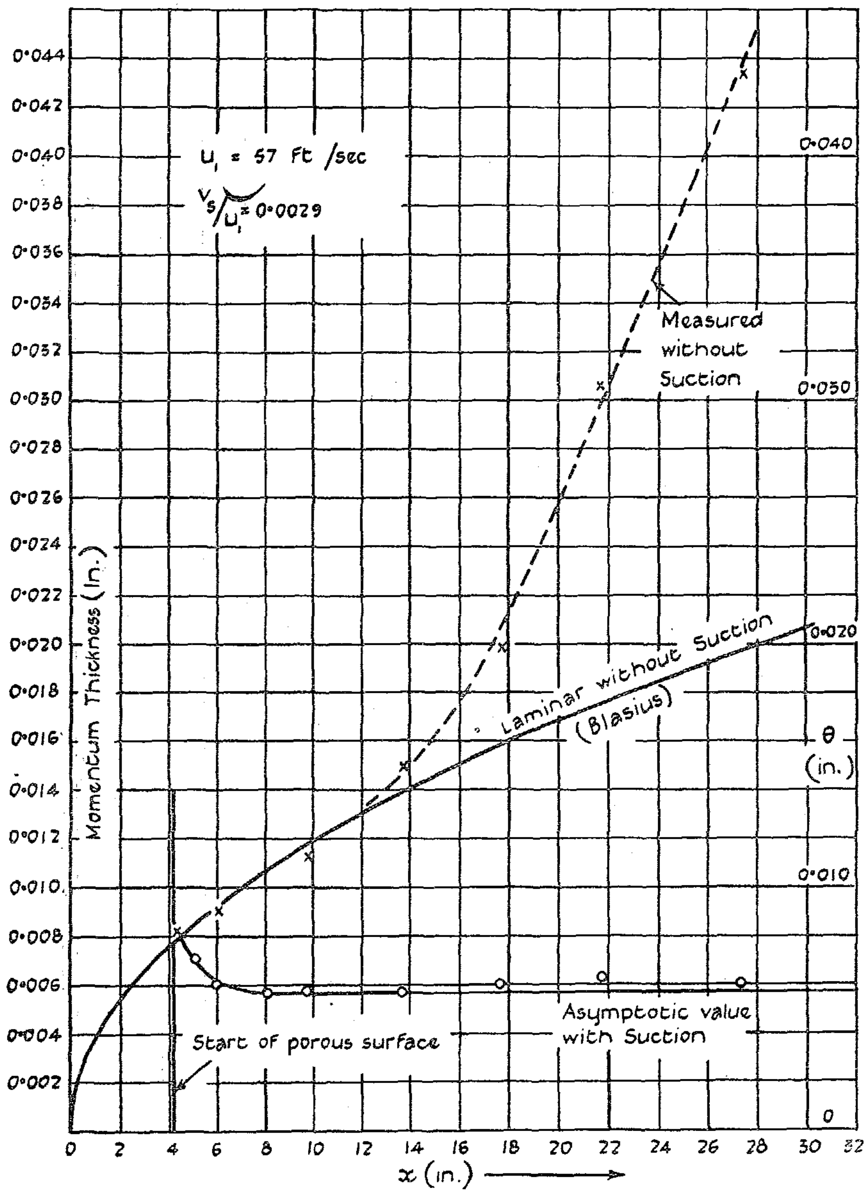

FIG. 12. Variation of momentum thickness.

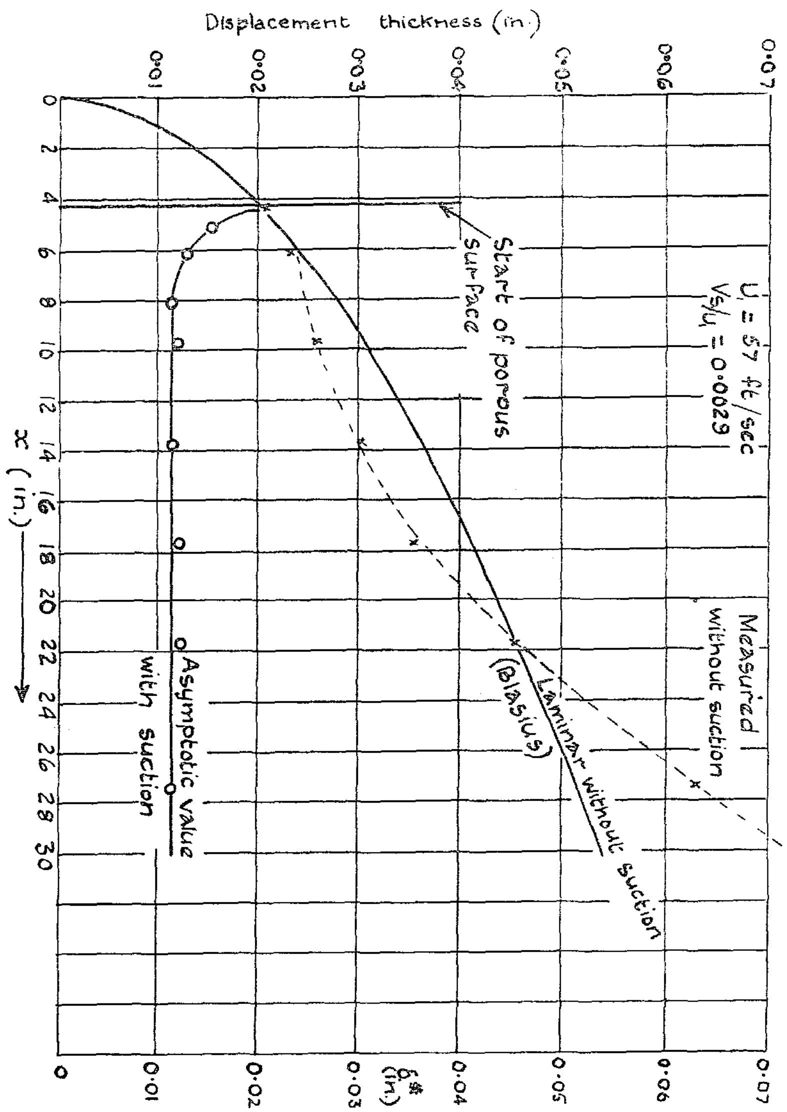

FIG. 11. Variation of displacement thickness.

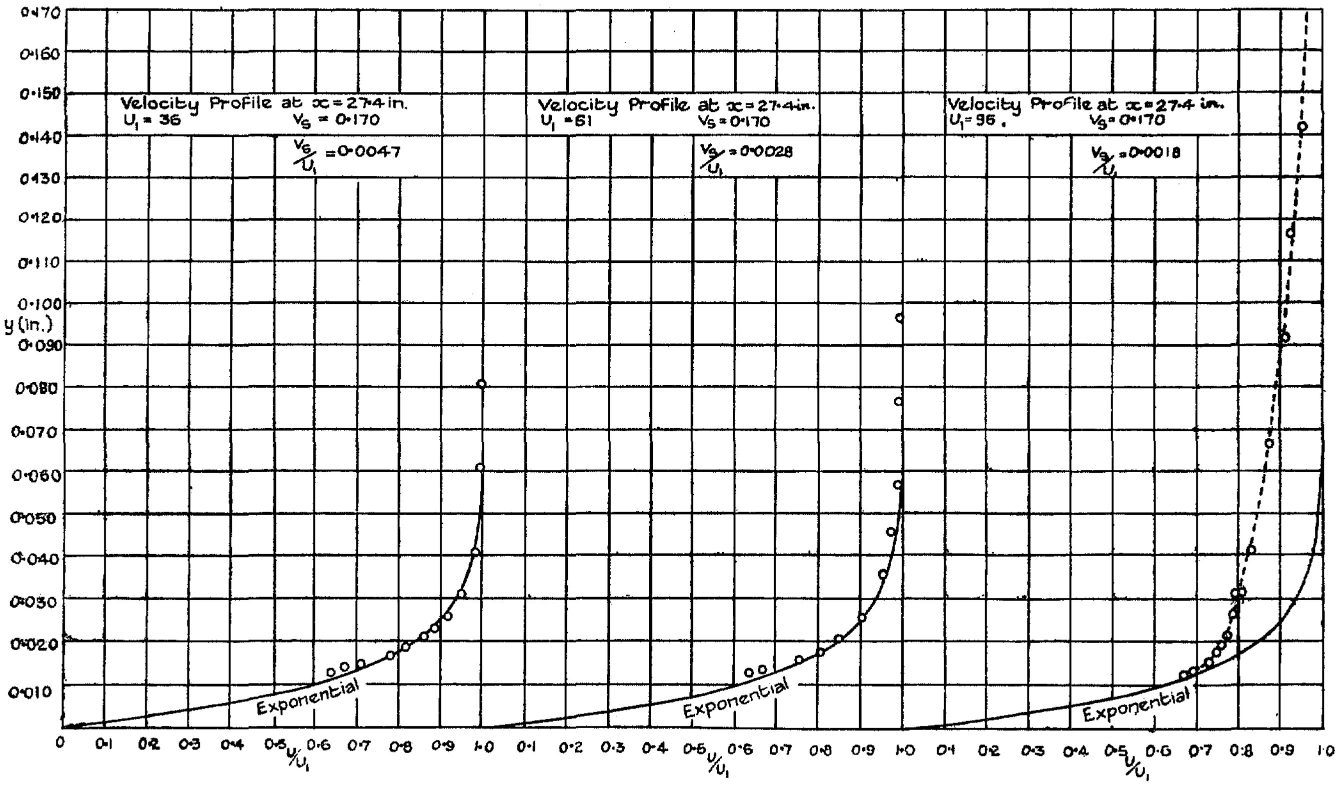

FIG. 13. FIG. 14. FIG. 15.

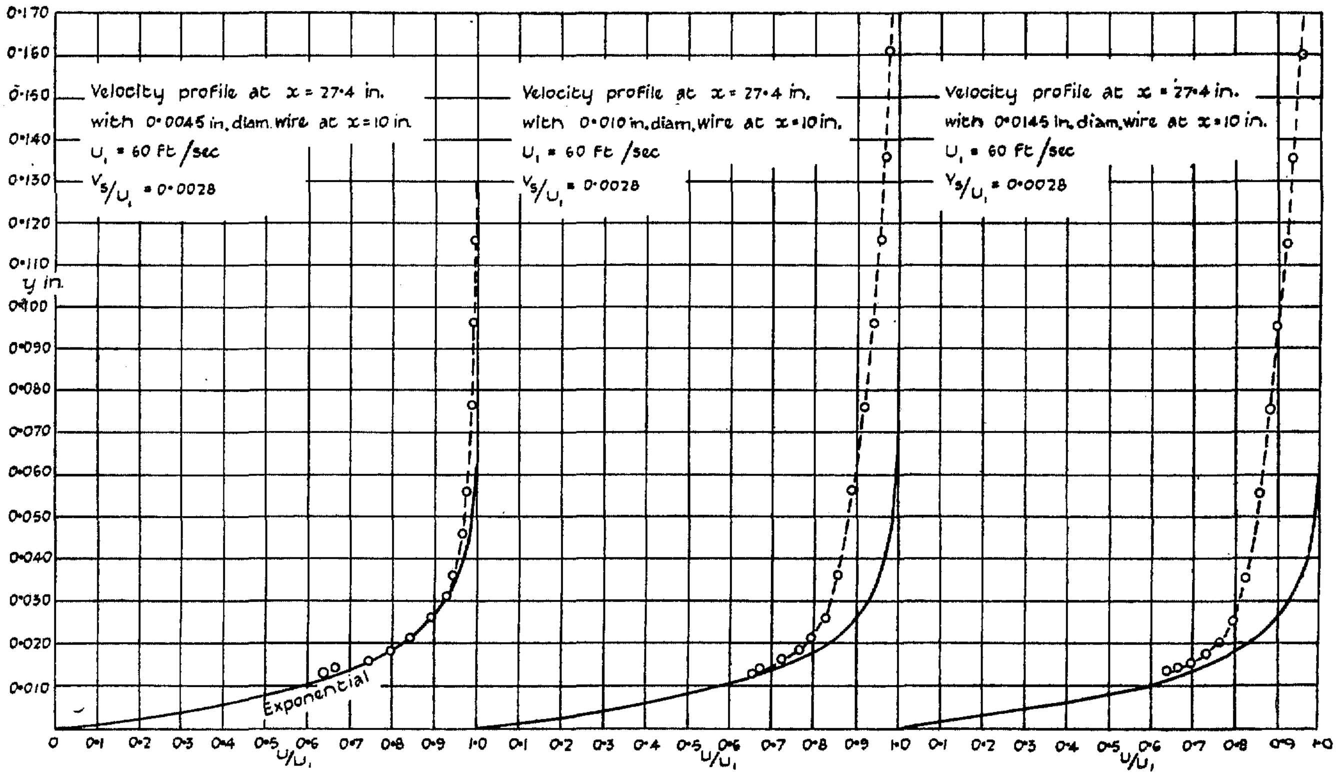

FIG. 16. FIG. 17. FIG. 18.

(22309) B*

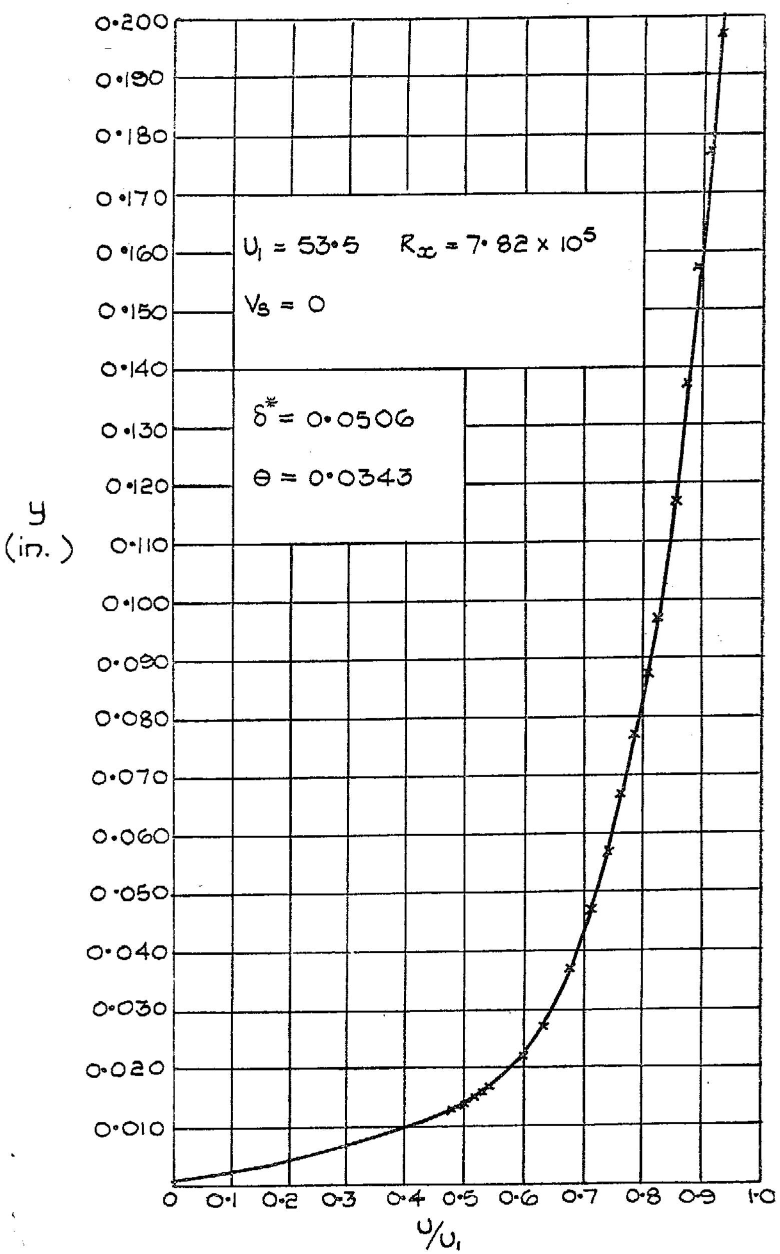
$U_1 = 53{\cdot}5$ $R_x = 7{\cdot}82 \times 10^5$
$V_s = 0$
$\delta^* = 0{\cdot}0506$
$\theta = 0{\cdot}0343$
y (in.)
0·010 0·020 0·030 0·040 0·050 0·060 0·070 0·080 0·090 0·100 0·110 0·120 0·130 0·140 0·150 0·160 0·170 0·180 0·190 0·200
0 0·1 0·2 0·3 0·4 0·5 0·6 0·7 0·8 0·9 1·0
u/U_1

FIG. 19.

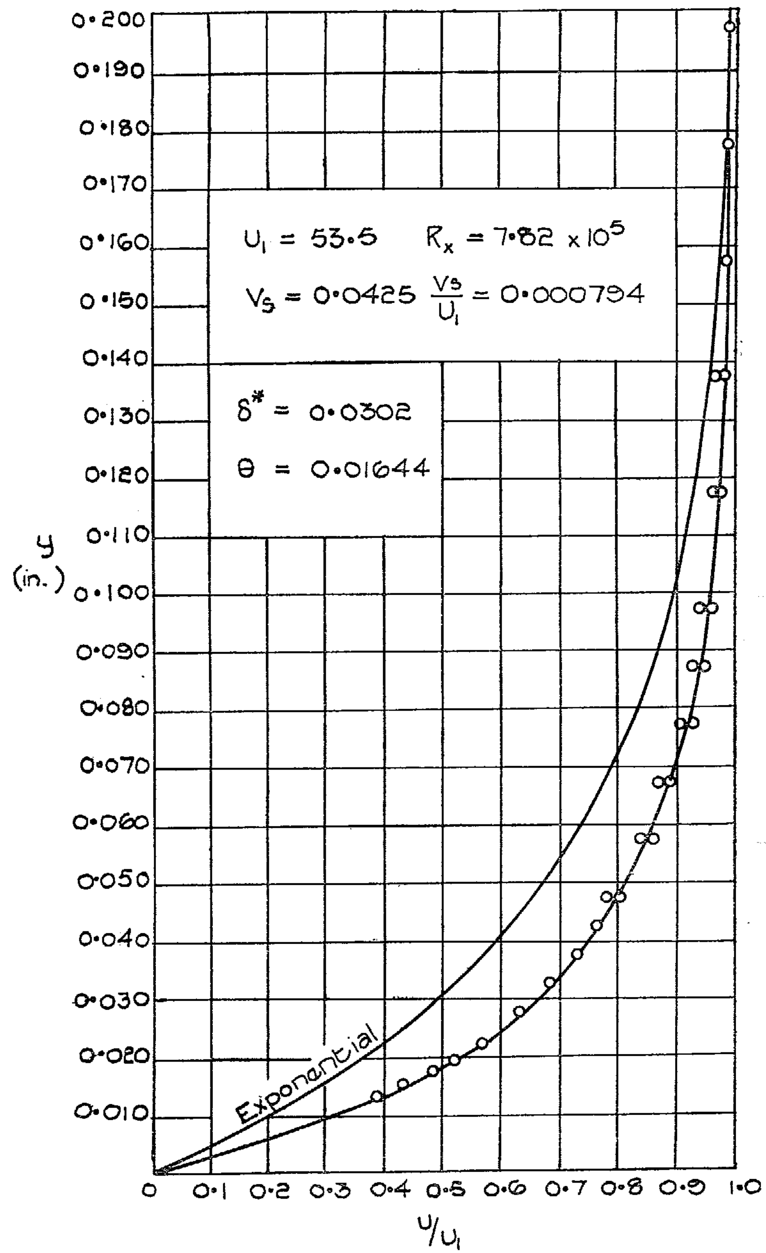
$U_1 = 53{\cdot}5$ $R_x = 7{\cdot}82 \times 10^5$
$V_s = 0{\cdot}0425$ $\frac{V_s}{U_1} = 0{\cdot}000794$
$\delta^* = 0{\cdot}0302$
$\theta = 0{\cdot}01644$
Exponential
y (in.)
0·010 0·020 0·030 0·040 0·050 0·060 0·070 0·080 0·090 0·100 0·110 0·120 0·130 0·140 0·150 0·160 0·170 0·180 0·190 0·200
0 0·1 0·2 0·3 0·4 0·5 0·6 0·7 0·8 0·9 1·0
u/U_1

FIG. 20.

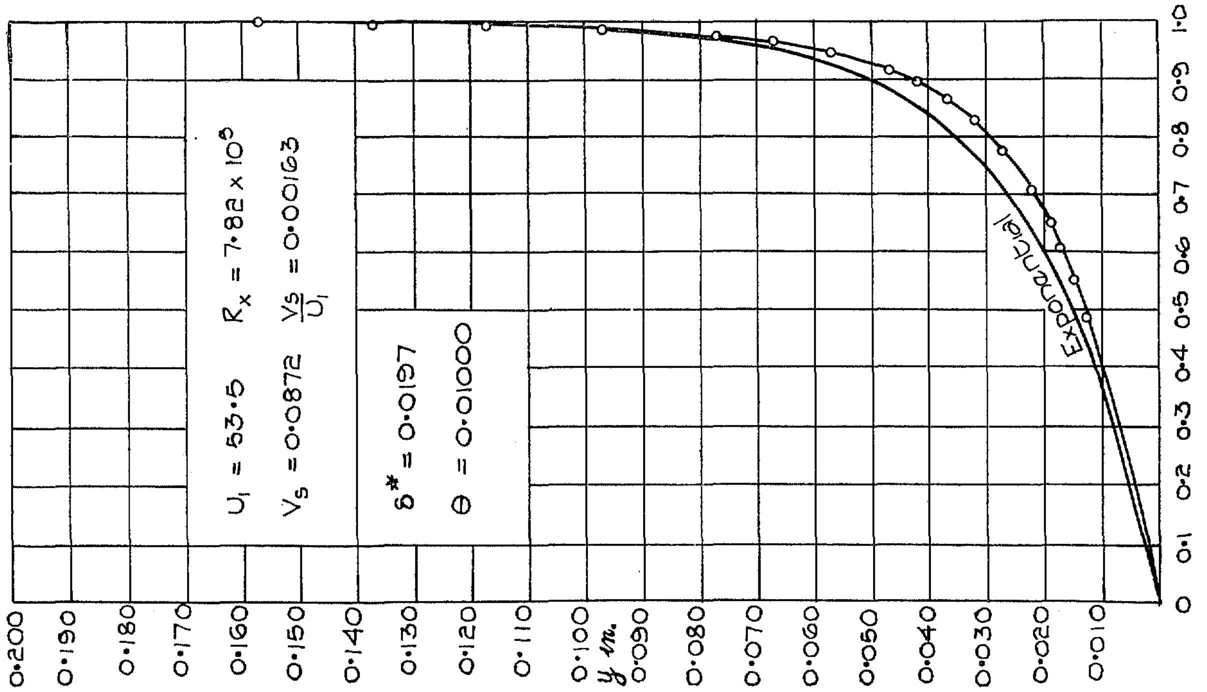

FIG. 21.

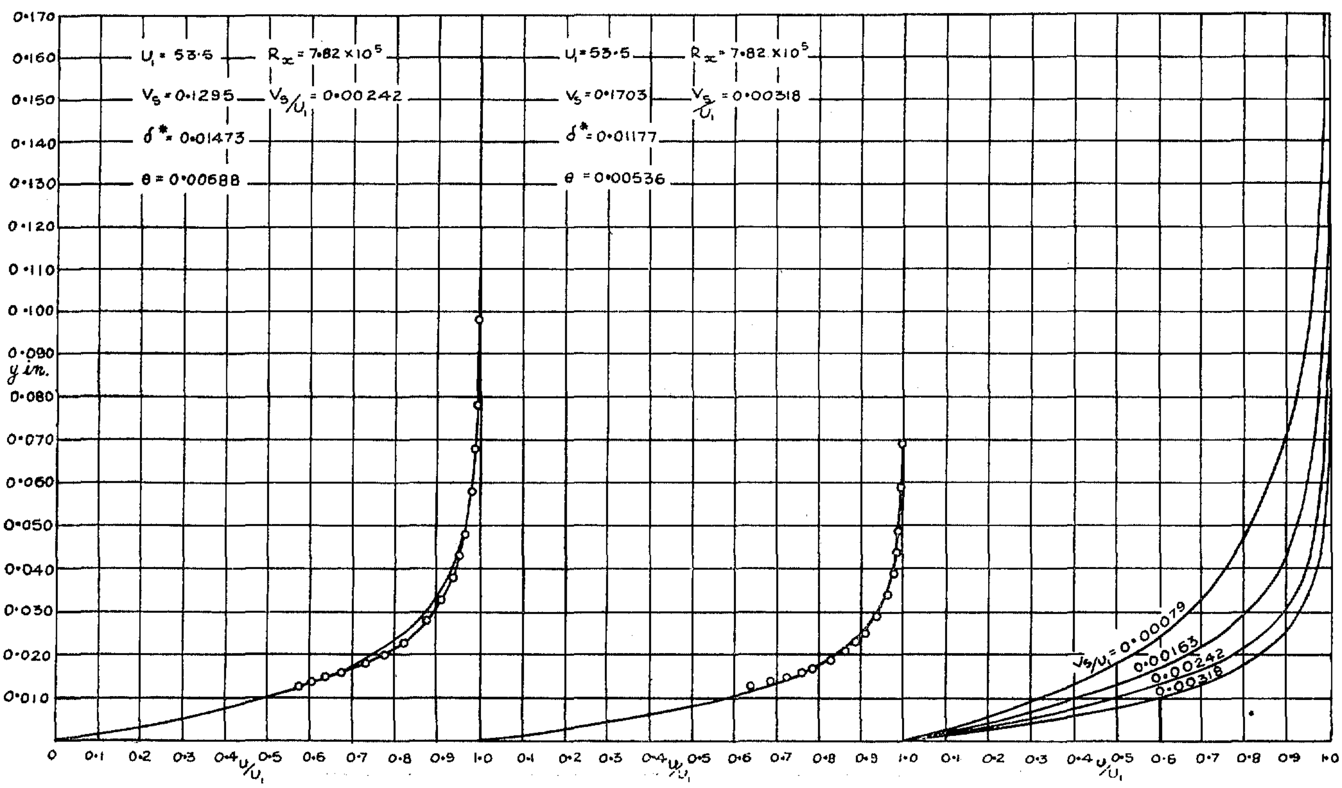

FIG. 22. FIG. 23. FIG. 24.

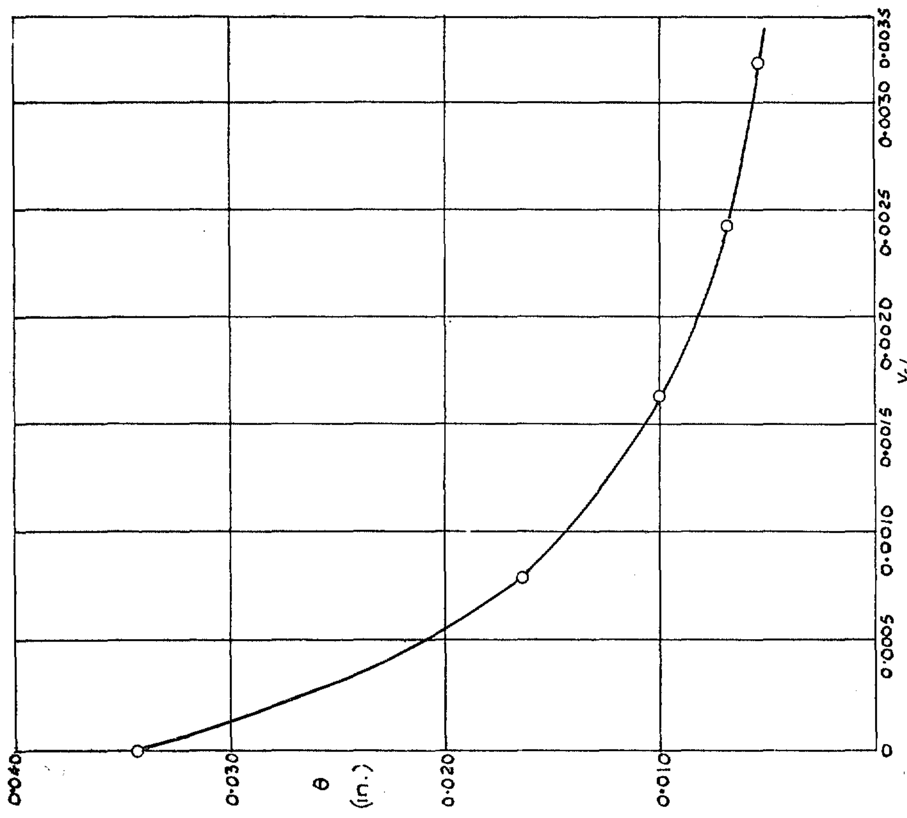

FIG. 25. Variation of momentum thickness with v_s/U_1.

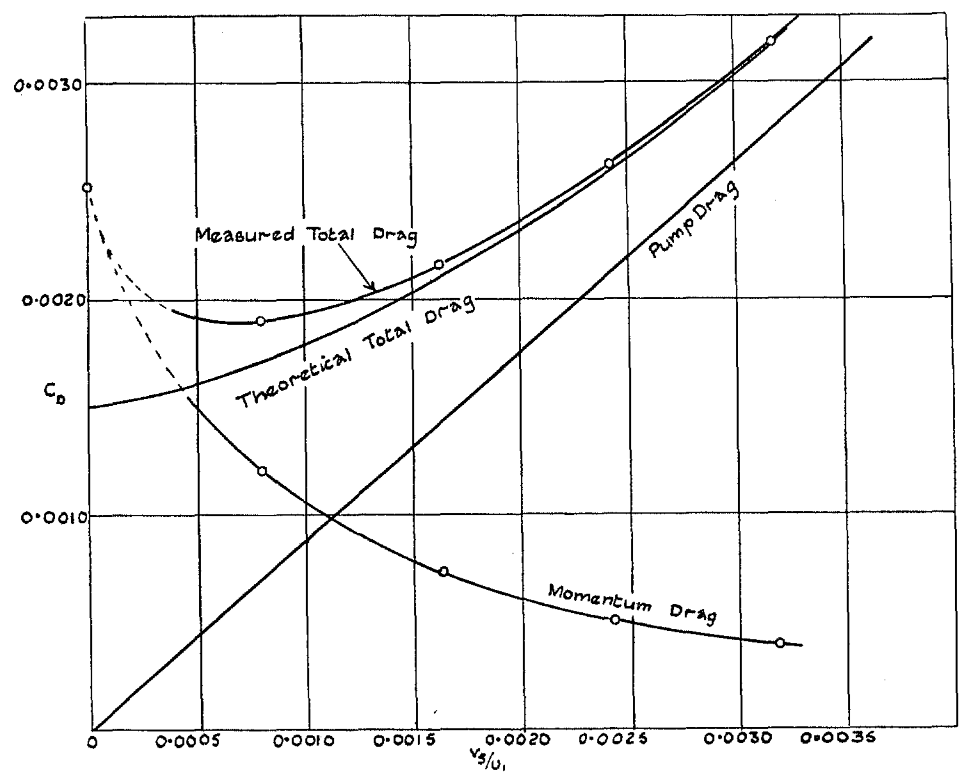

FIG. 26. Variation of drag with suction velocity.

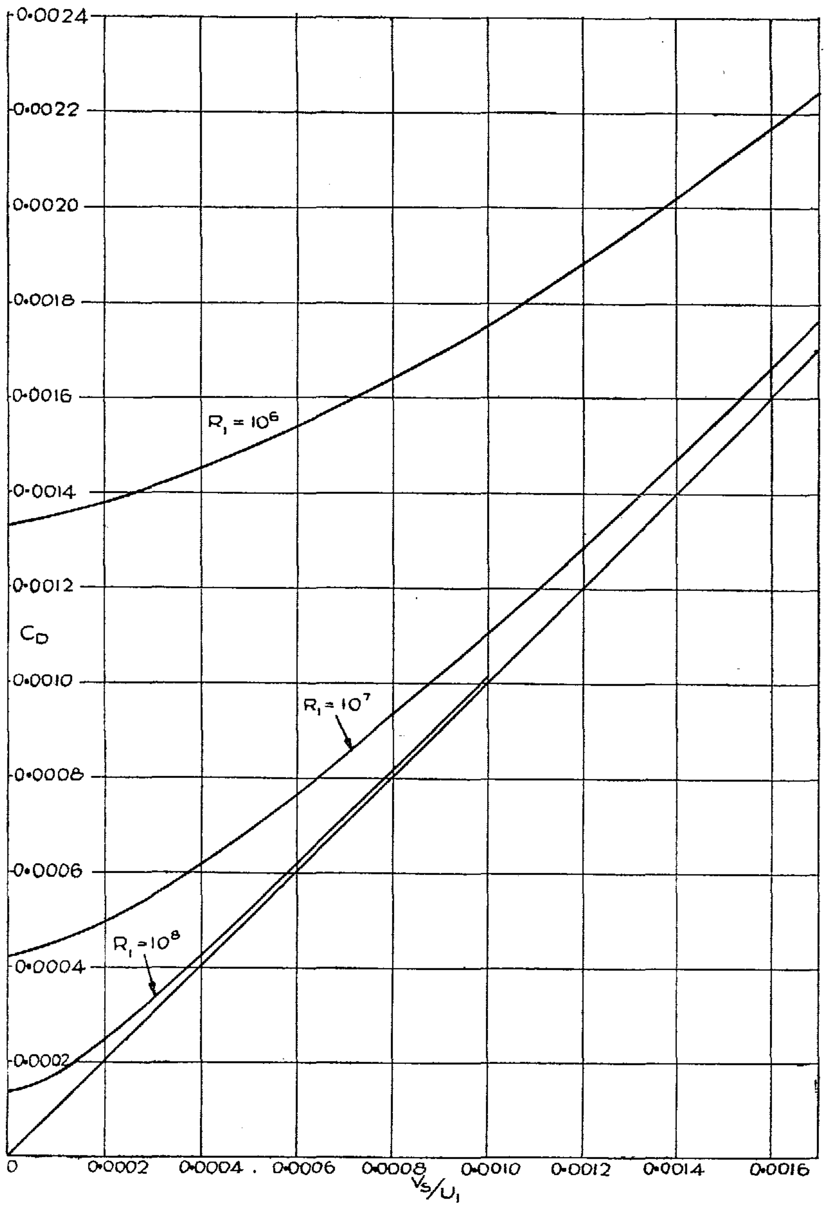

FIG. 27. Theoretical variation of total-drag coefficient with v_s/U_1 at different Reynolds number (suction starting at leading edge).

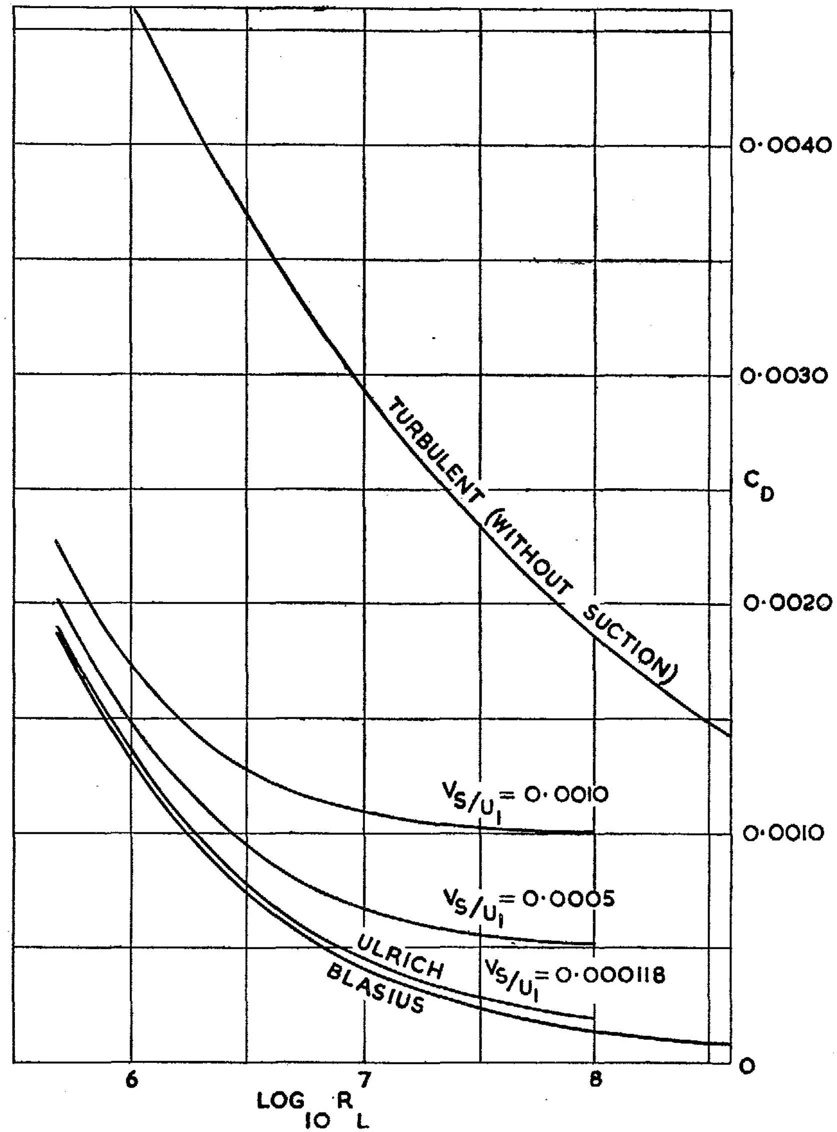

FIG. 28. Theoretical variation of total-drag coefficient with Reynolds number (suction starting at leading edge).

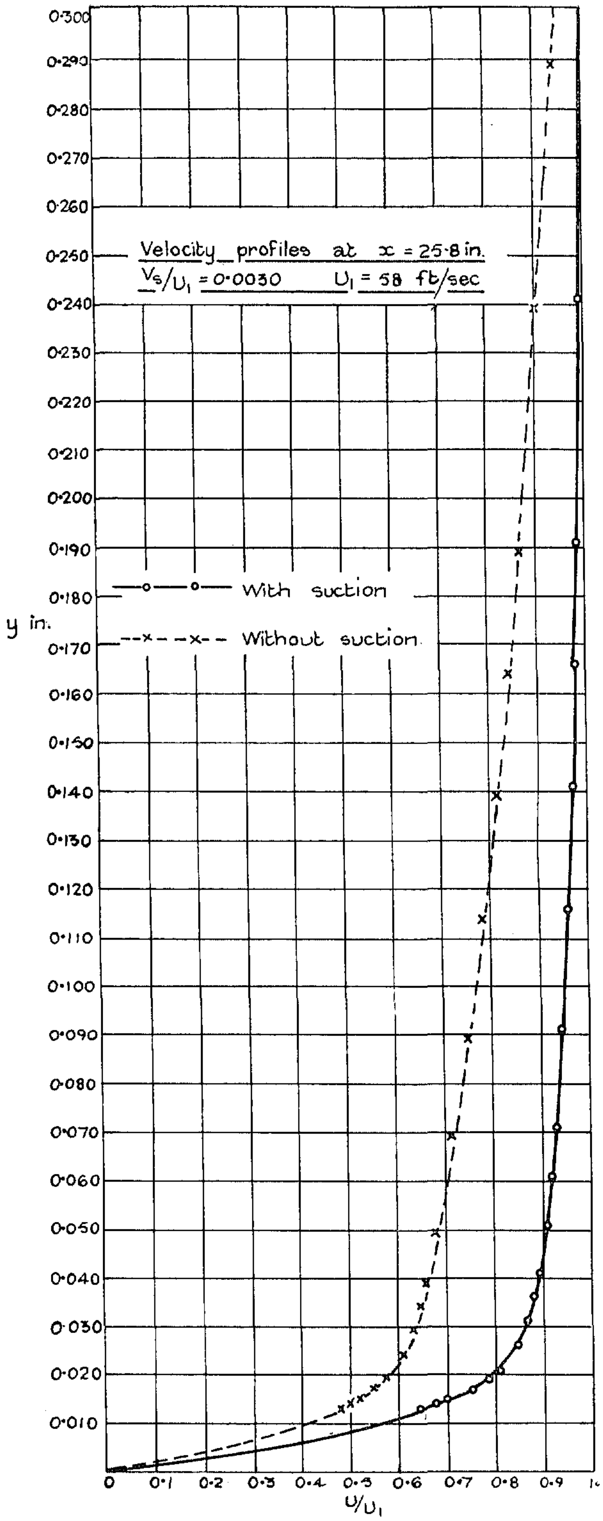

Velocity profiles at x = 25·8 in.
Vs/U1 = 0·0030 U1 = 58 ft/sec
With suction
Without suction
y in.
U/U1

FIG. 29.

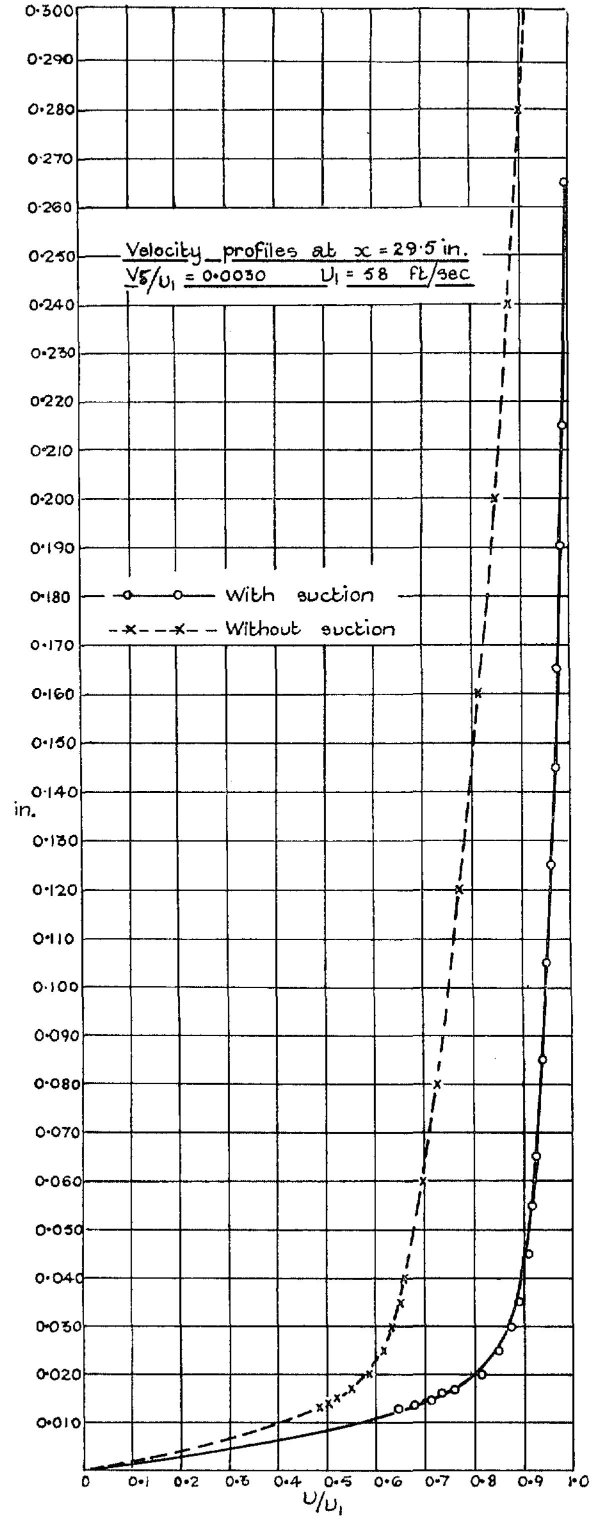

Velocity profiles at x = 29·5 in.
Vs/U1 = 0·0030 U1 = 58 ft/sec
With suction
Without suction
in.
U/U1

FIG. 30.

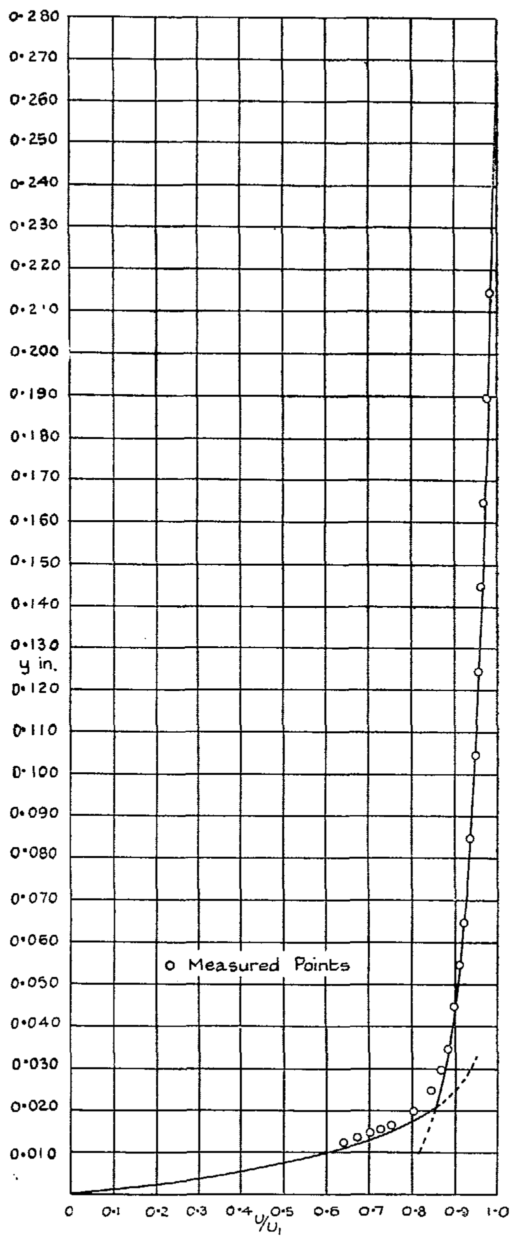

FIG. 32. Calculated asymptotic profile for turbulent flow at $v_s/U_1 = 0 \cdot 0030$. $U_1 = 58$ ft/sec.

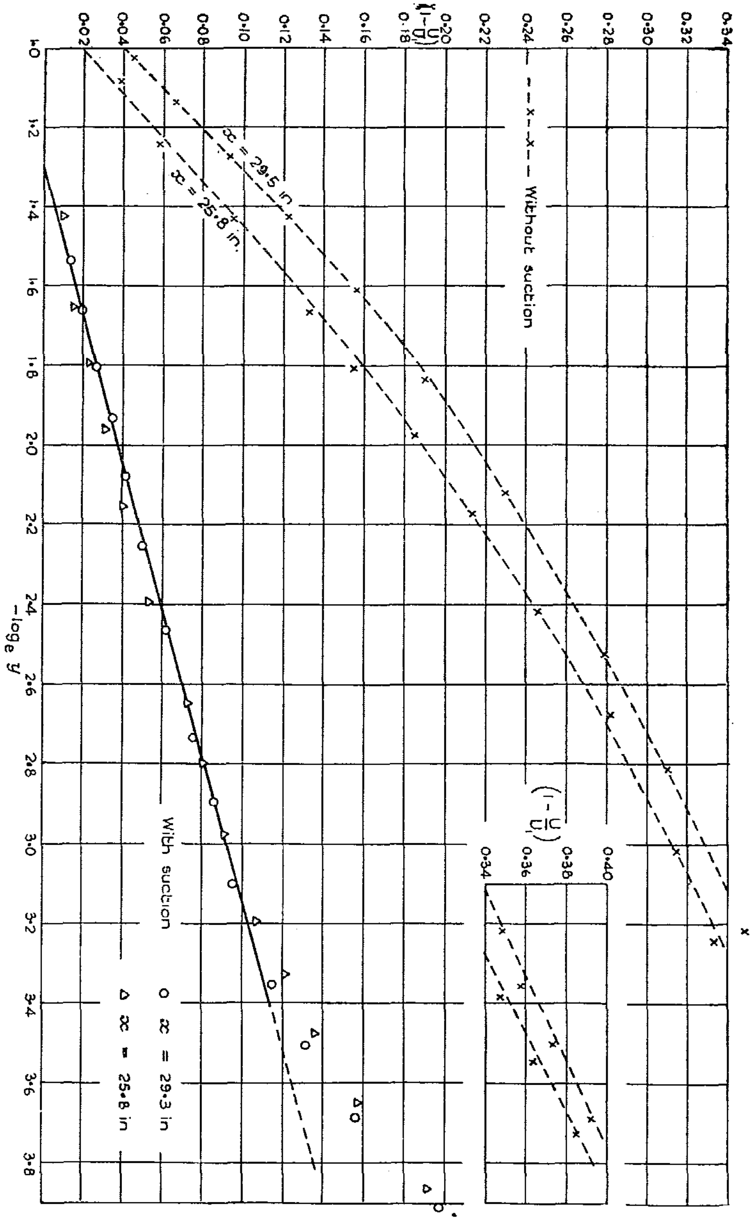

FIG. 31.

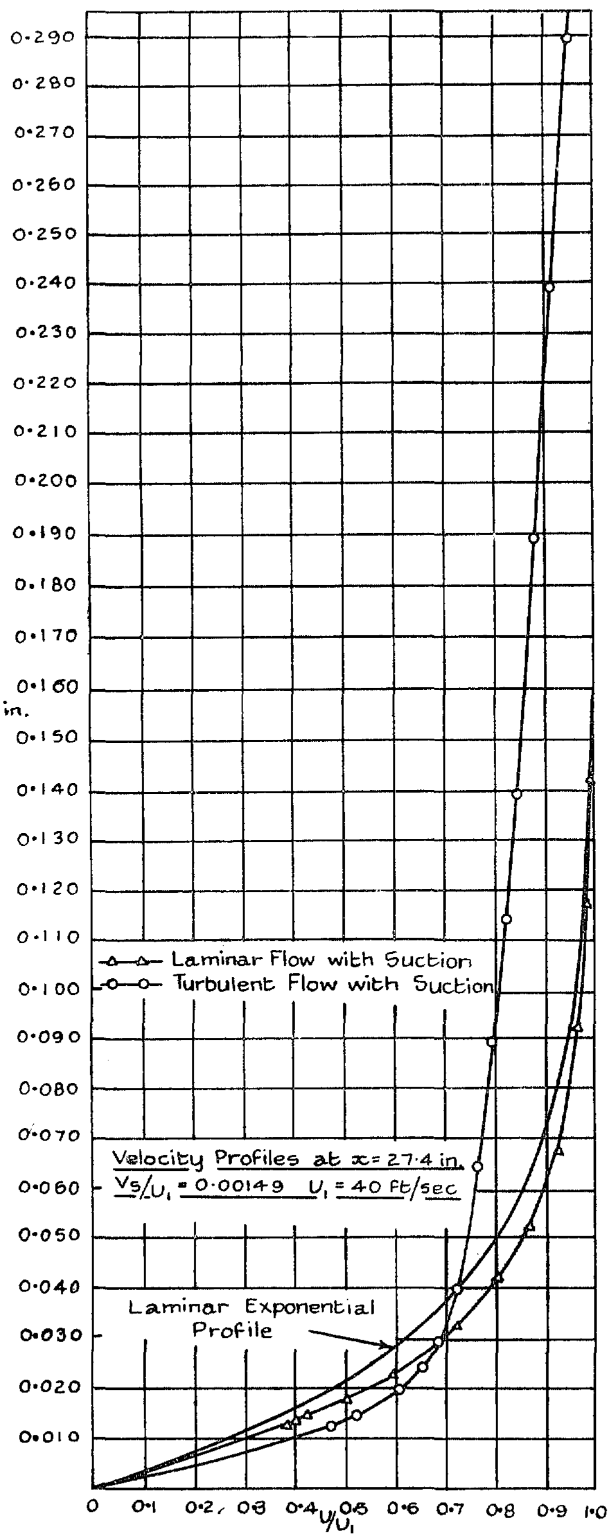
Laminar Flow with Suction
Turbulent Flow with Suction
Velocity Profiles at x = 27·4 in.
Vs/U₁ = 0·00149 U₁ = 40 ft/sec
Laminar Exponential Profile
in.
U/U₁

FIG. 33.

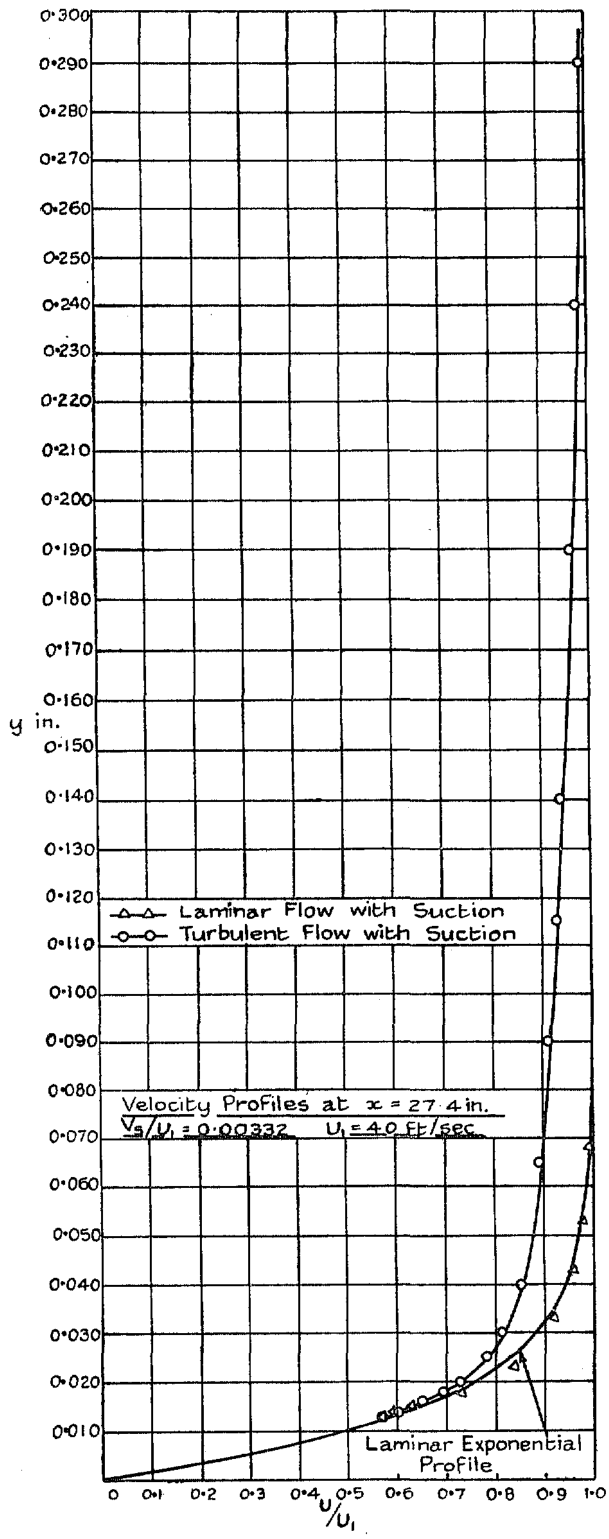
y in.
Laminar Flow with Suction
Turbulent Flow with Suction
Velocity Profiles at x = 27·4 in.
Vs/U₁ = 0·00332 U₁ = 40 ft/sec
Laminar Exponential Profile
U/U₁

FIG. 34.

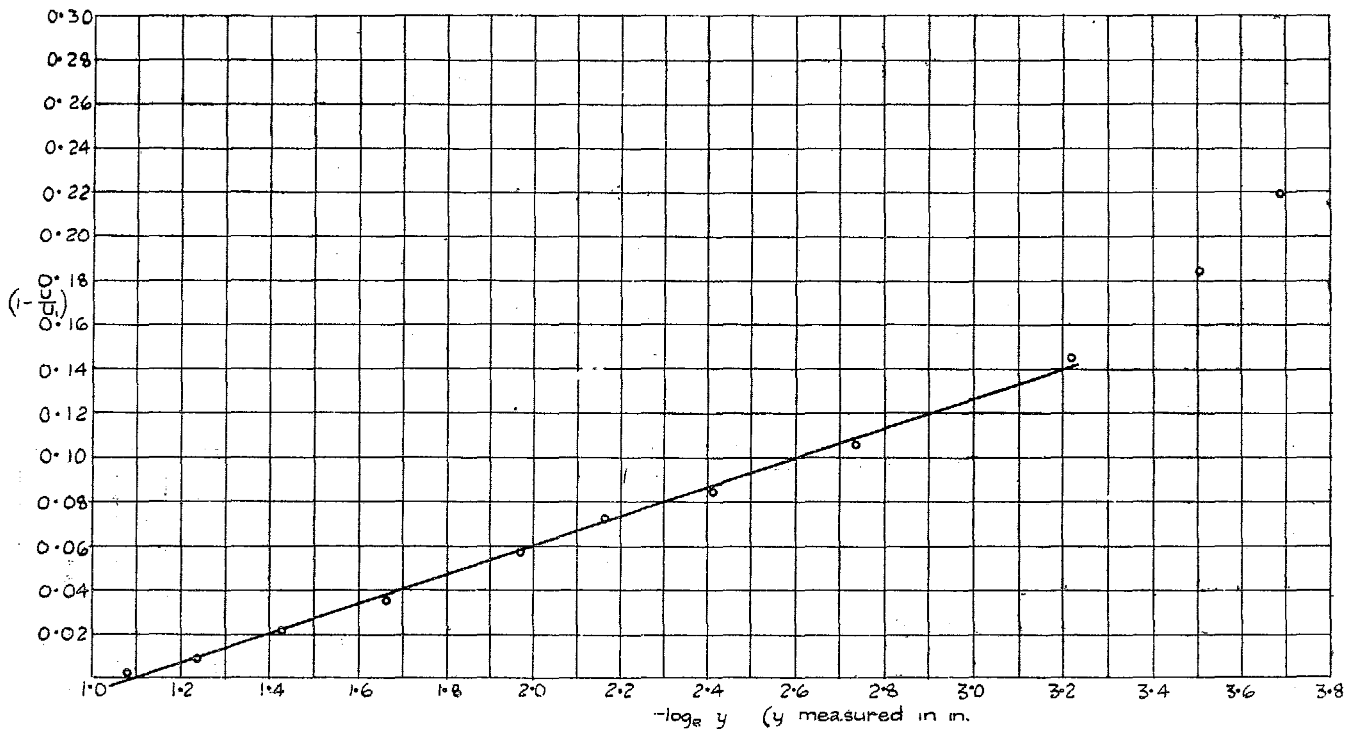

FIG. 35. Plot of $(1 - U/U\ )$ against $-\log_e y$ for the turbulent profile of Fig. 34.

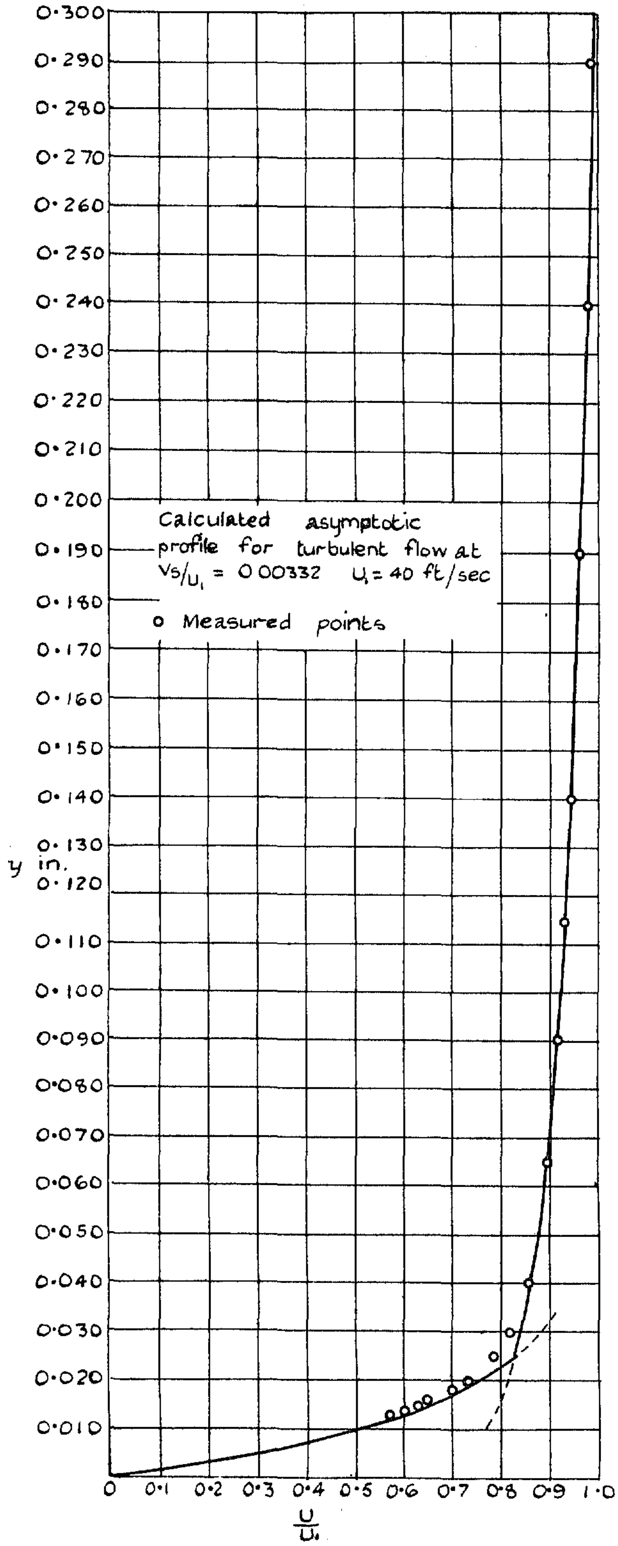

FIG. 36.

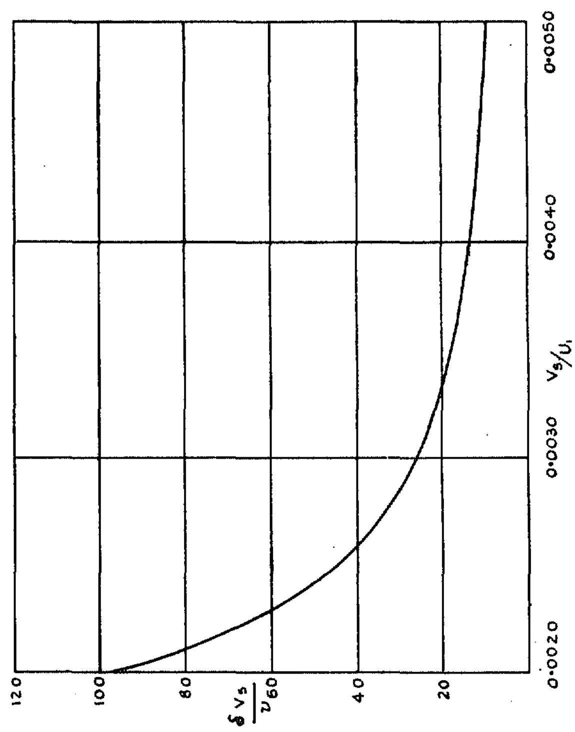

FIG. 37. Calculated variation of asymptotic thickness for turbulent boundary layer.

(22309) Wt. 15-680 K9 5/53 F. M. & S.

PRINTED IN GREAT BRITAIN

R. & M. No. 2628
(11,476, 12,193)
A.R.C. Technical Report

Publications of the Aeronautical Research Council

ANNUAL TECHNICAL REPORTS OF THE AERONAUTICAL RESEARCH COUNCIL (BOUND VOLUMES)

1936 Vol. I. Aerodynamics General, Performance, Airscrews, Flutter and Spinning. 40*s.* (40*s.* 9*d.*)
Vol. II. Stability and Control, Structures, Seaplanes, Engines, etc. 50*s.* (50*s.* 10*d.*)

1937 Vol. I. Aerodynamics General, Performance, Airscrews, Flutter and Spinning. 40*s.* (40*s.* 10*d.*)
Vol. II. Stability and Control, Structures, Seaplanes, Engines, etc. 60*s.* (61*s.*)

1938 Vol. I. Aerodynamics General, Performance, Airscrews. 50*s.* (51*s.*)
Vol. II. Stability and Control, Flutter, Structures, Seaplanes, Wind Tunnels, Materials. 30*s.* (30*s.* 9*d.*)

1939 Vol. I. Aerodynamics General, Performance, Airscrews, Engines. 50*s.* (50*s.* 11*d.*)
Vol. II. Stability and Control, Flutter and Vibration, Instruments, Structures, Seaplanes, etc. 63*s.* (64*s.* 2*d.*)

1940 Aero and Hydrodynamics, Aerofoils, Airscrews, Engines, Flutter, Icing, Stability and Control, Structures, and a miscellaneous section. 50*s.* (51*s.*)

1941 Aero and Hydrodynamics, Aerofoils, Airscrews, Engines, Flutter, Stability and Control, Structures. 63*s.* (64*s.* 2*d.*)

1942 Vol. I. Aero and Hydrodynamics, Aerofoils, Airscrews, Engines. 75*s.* (76*s.* 3*d.*)
Vol. II. Noise, Parachutes, Stability and Control, Structures, Vibration, Wind Tunnels. 47*s.* 6*d.* (48*s.* 5*d.*)

1943 Vol. I. (In the press.)
Vol. II. (In the press.)

ANNUAL REPORTS OF THE AERONAUTICAL RESEARCH COUNCIL—

1933-34	1*s.* 6*d.* (1*s.* 8*d.*)	1937	2*s.* (2*s.* 2*d.*)
1934-35	1*s.* 6*d.* (1*s.* 8*d.*)	1938	1*s.* 6*d.* (1*s.* 8*d.*)
April 1, 1935 to Dec. 31, 1936.	4*s.* (4*s.* 4*d.*)	1939-48	3*s.* (3*s.* 2*d.*)

INDEX TO ALL REPORTS AND MEMORANDA PUBLISHED IN THE ANNUAL TECHNICAL REPORTS AND SEPARATELY—

April, 1950 - - - - - R. & M. No. 2600. 2*s.* 6*d.* (2*s.* 7½*d.*)

AUTHOR INDEX TO ALL REPORTS AND MEMORANDA OF THE AERONAUTICAL RESEARCH COUNCIL—

1909-1949 - - - - - R. & M. No. 2570. 15*s.* (15*s.* 3*d.*)

INDEXES TO THE TECHNICAL REPORTS OF THE AERONAUTICAL RESEARCH COUNCIL—

December 1, 1936—June 30, 1939.	R. & M. No. 1850.	1*s.* 3*d.* (1*s.* 4½*d.*)
July 1, 1939—June 30, 1945.	R. & M. No. 1950.	1*s.* (1*s.* 1½*d.*)
July 1, 1945—June 30, 1946.	R. & M. No. 2050.	1*s.* (1*s.* 1½*d.*)
July 1, 1946—December 31, 1946.	R. & M. No. 2150.	1*s.* 3*d.* (1*s.* 4½*d.*)
January 1, 1947—June 30, 1947.	R. & M. No. 2250.	1*s.* 3*d.* (1*s.* 4½*d.*)
July, 1951. - - - - -	R. & M. No. 2350.	1*s.* 9*d.* (1*s.* 10½*d.*)

Prices in brackets include postage.

Obtainable from

HER MAJESTY'S STATIONERY OFFICE

York House, Kingsway, London, W.C.2; 423 Oxford Street, London, W.1 (Post Orders: P.O. Box 569, London, S.E.1); 13a Castle Street, Edinburgh 2; 39 King Street, Manchester 2; 2 Edmund Street, Birmingham 3; 1 St. Andrew's Crescent, Cardiff; Tower Lane, Bristol 1; 80 Chichester Street, Belfast or through any bookseller.

S.O. Code No. 23-2628